JGR Biogeosciences

RESEARCH ARTICLE
10.1029/2021JG006573

Tidal and Nontidal Marsh Restoration: A Trade-Off Between Carbon Sequestration, Methane Emissions, and Soil Accretion

Ariane Arias-Ortiz[1,2], Patricia Y. Oikawa[3], Joseph Carlin[4], Pere Masqué[5,6,7], Julie Shahan[3], Sadie Kanneg[4], Adina Paytan[2], and Dennis D. Baldocchi[1]

[1]Ecosystem Science Division, Department of Environmental Science, Policy and Management, University of California, Berkeley, CA, USA, [2]Institute of Marine Sciences, University of California, Santa Cruz, CA, USA, [3]Department of Earth and Environmental Sciences, California State University, East Bay, Hayward, CA, USA, [4]Department of Geological Sciences, California State University, Fullerton, CA, USA, [5]Departament de Física & Institut de Ciència i Tecnologia Ambientals, Universitat Autònoma de Barcelona, Bellaterra, Spain, [6]School of Natural Sciences, Centre for Marine Ecosystems Research, Edith Cowan University, Joondalup, WA, Australia, [7]International Atomic Energy Agency, Principality of Monaco, Monaco

Abstract Support for coastal wetland restoration projects that consider carbon (C) storage as a climate mitigation benefit is growing as coastal wetlands are sites of substantial C sequestration. However, the climate footprint of wetland restoration remains controversial as wetlands can also be large sources of methane (CH_4). We quantify the vertical fluxes of C in restored fresh and oligohaline nontidal wetlands with managed hydrology and a tidal euhaline marsh in California's San Francisco Bay-Delta. We combine the use of eddy covariance atmospheric flux measurements with ^{210}Pb-derived soil C accumulation rates to quantify the C sequestration efficiency of restored wetlands and their associated climate mitigation service. Nontidal managed wetlands were the most efficient in burying C on-site, with soil C accumulation rates as high as their net atmospheric C uptake (-280 ± 90 and -350 ± 150 g C m^{-2} yr^{-1}). In contrast, the restored tidal wetland exhibited lower C burial rates over decadal timescales (70 ± 19 g C m^{-2} yr^{-1}) that accounted for ~13%–23% of its annual C uptake, suggesting that the remaining fraction is exported via lateral hydrologic flux. From an ecosystem radiative balance perspective, the restored tidal wetland showed a > 10 times higher CO_2-sequestration to CH_4-emission ratio than the nontidal managed wetlands. Thus overall, tidal wetland restoration resulted in a negative radiative forcing (cooling) through increased soil C accumulation, while nontidal wetland restoration led to an early positive forcing (warming) through increased CH_4 emissions potentially lasting between 2.1 ± 2.0 to 8 ± 4 decades.

Plain Language Summary Coastal wetlands have great potential to remove carbon dioxide from the atmosphere and mitigate climate change. This study aims to understand how effectively restored wetlands bury carbon in soils and sequester it, and the extent to which they produce methane, a potent greenhouse gas. We measured how much carbon dioxide and methane flow into and out of three restored wetlands differing in their restoration design, salinity, and tidal influence. We found that most of the carbon dioxide removed from the atmosphere by nontidal wetlands was stored in their soils, while restored tidal wetland soils stored a smaller fraction (13%–23%) of the removed carbon. Despite the lower carbon sequestration efficiency, the restored tidal wetland was a greater greenhouse gas sink and climate intervention because it emitted very little methane. Methane emissions in nontidal freshwater and brackish marshes fully offset the carbon dioxide removed via carbon burial for roughly the first 2–8 decades, while the tidal wetland contributed to greenhouse gas removal immediately after restoration. The merits of nontidal managed wetland restoration lie in increased soil and C accretion, but it should not be assumed that soil carbon storage results in an immediate climate mitigation benefit.

Key Points:

- Net atmospheric C uptake and soil C accumulation rates were equivalent measures of C sequestration in nontidal managed wetlands
- Managed wetlands showed the largest C accumulation but had lower CO_2-sequestration to CH_4-emission ratios than the restored tidal wetland
- Nontidal wetland restoration resulted in an early warming effect, while tidal restoration resulted in immediate climatic cooling

Supporting Information:

Supporting Information may be found in the online version of this article.

Correspondence to:

A. Arias-Ortiz,
aariasortiz@berkeley.edu

Citation:

Arias-Ortiz, A., Oikawa, P. Y., Carlin, J., Masqué, P., Shahan, J., Kanneg, S., et al. (2021). Tidal and nontidal marsh restoration: A trade-off between carbon sequestration, methane emissions, and soil accretion. *Journal of Geophysical Research: Biogeosciences*, *126*, e2021JG006573. https://doi.org/10.1029/2021JG006573

Received 6 AUG 2021
Accepted 3 NOV 2021

Author Contributions:

Conceptualization: Ariane Arias-Ortiz, Joseph Carlin, Dennis D. Baldocchi
Data curation: Ariane Arias-Ortiz, Julie Shahan
Formal analysis: Ariane Arias-Ortiz
Funding acquisition: Ariane Arias-Ortiz, Patricia Y. Oikawa, Pere Masqué, Adina Paytan, Dennis D. Baldocchi
Investigation: Ariane Arias-Ortiz, Joseph Carlin, Pere Masqué, Julie Shahan, Sadie Kanneg
Methodology: Ariane Arias-Ortiz, Joseph Carlin, Dennis D. Baldocchi
Project Administration: Ariane Arias-Ortiz

1. Introduction

Coastal wetlands are sites of high carbon (C) sequestration rates through continuous vertical accretion owing to both, their capacity to trap allochthonous sediments and the allocation of a large fraction of their production to roots and rhizomes (Duarte et al., 2013). Their high rates of photosynthetic C fixation and the low rates of organic matter decomposition in their waterlogged and oxygen-poor soils promote the preservation

Resources: Ariane Arias-Ortiz, Patricia Y. Oikawa, Joseph Carlin, Pere Masqué, Adina Paytan, Dennis D. Baldocchi
Supervision: Patricia Y. Oikawa, Adina Paytan, Dennis D. Baldocchi
Visualization: Ariane Arias-Ortiz
Writing – original draft: Ariane Arias-Ortiz
Writing – review & editing: Patricia Y. Oikawa, Joseph Carlin, Pere Masqué, Julie Shahan, Adina Paytan, Dennis D. Baldocchi

of large quantities of soil C (also known as Blue Carbon) for centuries to millennia, contributing to the long-term removal of carbon dioxide (CO_2) from the atmosphere. The accumulation of mineral and organic matter in their soils and the associated increase in soil volume and surface elevation (Morris et al., 2002) has allowed these ecosystems to persist for millennia of rising sea level (Kirwan & Megonigal, 2013), protecting the coastline against storm surges and rising tides. With global sea level projected to rise at an average rate ranging between 4 to 15 mm yr^{-1} through the twenty-first century (IPCC, 2019), support for coastal wetland restoration projects for both carbon storage and coastal protection is growing (Crooks et al., 2014; Fennessy & Lei, 2018; Sapkota & White, 2020) as coastal wetlands can act as net carbon sinks (Howard et al., 2017), provide flood control (Mitsch & Gossilink, 2000), and their restoration (Kroeger et al., 2017) and conservation (Griscom et al., 2017; Siikamaki et al., 2012) could reduce, mitigate or avoid future greenhouse gas emissions. However, the conditions that promote soil C storage in wetlands may lead to the production of methane (CH_4), particularly in freshwater and brackish systems with salinities <18 (Poffenbarger et al., 2011). Methane is a greenhouse gas roughly 30 times more potent than CO_2 over 100 years (Forster et al., 2007; Neubauer & Megonigal, 2015), and approximately half of global CH_4 emissions come from natural, human-created, and human-impacted aquatic ecosystems (Rosentreter et al., 2021). As a result, the climate footprint of coastal wetland restoration activities remains controversial (Hemes et al., 2018; Petrescu et al., 2015) since many sites may emit CH_4 at rates that exceed C sequestration in terms of CO_2 equivalents (Hemes et al., 2018; Rosentreter et al., 2018; Windham-Myers et al., 2018). Restoration projects can be designed, managed, or engineered to maximize C sequestration (Miller et al., 2008; Mitsch et al., 2014), however, the realization that coastal wetlands can also be large sources of methane (CH_4) has led to the need to reassess the utility of the soil C storage function as an immediate climate mitigation service.

Accounting of greenhouse gas fluxes in coastal wetland ecosystems is of increasing interest to assess C mitigation benefits. Restoration projects can convert such benefits into carbon credits under existing global standards such as the VM0003 Methodology for Tidal Wetland and Seagrass Restoration (Emmer et al., 2015), or local methodologies like the American Carbon Registry's standard for the restoration of California Deltaic and coastal wetlands (Deverel et al., 2017). Common and affordable methods used to estimate changes in CO_2 emissions involve quantification of C stock changes in biomass and soils, the use of chronosequence data, or the radiometric dating of soils to determine average C accumulation rates over the lifetime of key radioisotopes, for example, ^{137}Cs (~70 years) and ^{210}Pb (~100 years) (Chmura et al., 2003). Soil C accumulation rates are often used as a proxy for the net wetland ecosystem C balance (NECB) as they represent the balance between C inputs (through photosynthesis or allochthonous C deposition) and losses (through respiration to CO_2 and CH_4 or hydrologic export) (Bogard et al., 2020; Forbrich et al., 2018; Keller, 2018). However, quantifying the climate-benefits of coastal wetland restoration projects using the approaches mentioned above is often challenging, because the rate of change of soil C stocks is generally slow, C stocks and accumulation rate estimates are limited in spatial scale and sampling frequency, nor are they adept at sampling the production of CH_4 and the hydrologic export of C.

The eddy covariance (EC) method (Baldocchi et al., 1988) is an alternative approach that provides direct and continuous measurements of greenhouse gas exchange between wetlands and the atmosphere at ecological- and management-relevant spatial scales (100–1,000 ha depending on tower height and wind dynamics). This method has been primarily used in terrestrial systems to study how ecosystem metabolism responds to a plethora of biophysical forcings (Baldocchi, 2020). However, the gradual reduction of sensor costs and its recent use on a few voluntary and compliance greenhouse gas quantification methodologies (Deverel et al., 2017) has led to the realization of its potential to improve C accounting in nature-based climate mitigation projects (Hemes et al., 2021). The continuous nature of EC flux measurements not only informs how C fluxes respond to interannual climate variability, management, and disturbance events (Chamberlain et al., 2020; Hemes et al., 2021) but can also provide information on the mechanisms controlling C uptake and emissions. This is particularly important for projections of C sequestration potential in the face of climate change. An important consideration to the application of the EC method in coastal systems, particularly those that are tidal, is that the atmospheric C exchange may not fully represent net C gains, as considerable amounts of C are exchanged laterally with adjacent water bodies rather than with the atmosphere (Bogard et al., 2020; Santos et al., 2021; Wang & Cai, 2004). The combination of discrete soil C accumulation rates estimated by using radionuclides with large-scale, high-frequency EC flux measurements has the potential to provide first-order estimates of the hydrologic C export (Bogard et al., 2020; Forbrich

et al., 2018), allowing the calculation of soil accretion and C accumulation rates relative to photosynthetic C fixation. The time scales captured by the two methods (i.e., soil C accumulation and EC estimates of atmospheric C fluxes) allow the study of C exchange patterns over representative timeframes; from sub-annual to decadal and to century as well as before and after restoration. Such data provide valuable information about the capacity of new restored coastal wetlands to keep pace with relative sea-level rise through biomass and soil accretion (Morris et al., 2002), improve estimates of NECB and biogeochemical models for soil C sequestration and emissions, and allow estimating changes in the radiative balance of the ecosystem with management, restoration, or disturbance.

With wetland restoration undertaken increasingly for the benefit of atmospheric CO_2 removal and storage in the soil, understanding the balance between C sequestration, CH_4 emissions, and hydrologic C loss is essential to our understanding of how restored or created wetlands will contribute to mitigating climate change. By coupling high-frequency EC land-atmosphere C flux measurements with soil accretion and C accumulation rates over a set of restored estuarine marshes differing in salinity, tidal influence, and landscape configuration, we quantify the stoichiometry of C sequestration, C emissions, and lateral C losses. Using a simple model of radiative forcing, atmospheric lifetimes, and marsh accretion (MEM) (Morris et al., 2002; Neubauer, 2014), we further discuss how the different restoration designs impact the greenhouse gas budget of restored wetlands and how this may change with climate change. From this analysis, we provide valuable information concerning the benefits and tradeoffs of coastal wetland restoration for climate change mitigation and adaptation.

2. Materials and Methods

2.1. Study Site

The study was conducted in California's San Francisco Bay-Delta (Bay-Delta) which, like other populated Deltas in the world, is sinking due to human activities (Ingebritsen et al., 2000; Syvitski et al., 2009). By 1950, all but ~10% of the Bay-Delta's 2,200 km^2 of historic wetland area was diked, drained, or filled for urbanization, agriculture, grazing, and salt production (Callaway et al., 2011) leading to massive loss of habitat for fish and wildlife, and severe land surface subsidence that continues to this day (Deverel et al., 2016; Deverel & Leighton, 2010; Drexler et al., 2018). In the 1970s, the world's first marsh restoration projects began in the Bay-Delta motivated by the desire to reverse the dire situation for native fishes, prevent flooding, and provide recreation areas (Goals Project, 1999). Most recently, the need to protect the region from sea-level rise and to reduce C emissions has further spurred major initiatives aimed at restoring extensive areas of diked or drained former tidal marshes (CDFW, 2020; Deverel et al., 2017; Goals Project, 2015), making the Bay-Delta a region rich in coastal wetland restoration and C storage projects from which lessons can be learned to benefit other projects nationally and globally.

Existing large-scale wetland restoration and management efforts in the Bay-Delta include tidal marsh restoration projects (e.g., South Bay Salt Pond Restoration Project) but also the construction of freshwater nontidal wetlands with managed hydrology at sites where the loss of elevation is too severe for tidal inundation and vegetation re-establishment (Callaway et al., 2011). The wetlands considered in this study include one restored tidal marsh and two nontidal restored marshes with managed hydrology (Table 1, Figure 1). The sites differ in salinity, tidal influence, surface elevation, and landscape configuration, and represent different restoration strategies to provide flood management, sea-level rise protection, reversal of land surface subsidence, C sequestration, and habitat for fish and wildlife. Individual study sites have been described in previous work and are summarized here (Chamberlain et al., 2018; Eichelmann et al., 2018; Hammond, 2016; Knox et al., 2015). All wetland sites experience a Mediterranean climate, with a long growing season from April to October that contrasts with the cold ocean water temperatures observed year-round (~12°C) (Vroom et al., 2017).

2.1.1. Tidal Wetland: Mount Eden Creek Marsh

Mount Eden Creek Marsh is a 75-ha restored tidal marsh located within the Eden Landing Ecological Reserve in South San Francisco Bay, CA, USA. The mean elevation at the site is 1.65 m NADV88 with a tidal range of 1.7 m and salinities above 30. The site is inundated twice daily by semidiurnal tides through Mount Eden Creek, with no upland action. Mount Eden Creek Marsh was restored from old industrial salt

Table 1
Summary Characteristics of Restored Wetland Sites

Site id	Location	Restoration year	Years of EC data included	Tidal influence	Salinity (ppt)	Wetland cover	Land-use history
Mount Eden Creek Marsh (US-EDN)	South San Francisco Bay 37.6156 N, 122.114 W	2011 vegetation planting 2008 tidal restoration	2018–2020	Tidal	30–35	Mudflat *Spartina foliosa* *Salicornia pacifica*	75 ha salt marsh restored from salt ponds
Mayberry (US-Myb)	Sherman Island 38.050 N, 121.765 W	2010	2012–2020	Nontidal, managed hydrology	1–9	*Typha* spp. *Phragmites* spp. *Schoenoplectus acutus* Open water	121 ha wetland restored from pepperweed and annual grassland pasture
West Pond (US-Tw1)	Twitchell Island 38.107 N, 121.647 W	1997	2013–2020	Nontidal, managed hydrology	0.1–0.3	*Typha* spp. *Schoenoplectus acutus*	3 ha wetland restored from a former corn field

evaporation ponds that operated from the late nineteenth century to the early 1970s (Stanford et al., 2013). Marsh vegetation was planted in 2011, 3 years after tidal restoration was initiated in 2008. The restoration process relied on tidal transport of sediment to rebuild the marsh plain and further tidal transport of seeds for vegetation development (Chapple, 2017). About 20% of the marsh area is currently vegetated by pickleweed (*Salicornia pacifica)* and cordgrass (*Spartina foliosa*) species, and 80% consists of mudflat areas. An EC tower that is part of the Ameriflux Network (US-EDN; Oikawa, 2020) is located at the site. Within the average tower footprint (this is the upwind area contributing to the measured fluxes), the landcover is roughly 70% mudflat and 30% vegetation.

2.1.2. Nontidal Wetlands With Managed Hydrology: Mayberry and West Pond

The two nontidal wetlands with managed hydrology in this study (hereafter, managed wetlands) are Mayberry (US-Myb; Hatala Matthes et al., 2021), a 121-ha marsh restored in 2010 on former grassland pasture, and West Pond (US-Tw1; Valach, Szutu, et al., 2021), a 3-ha marsh restored in 1997 on a former corn field. The two sites are located in the western portion of the Sacramento-San Joaquin Delta, on heavily subsided islands surrounded by levees at −3.73 and −3.17 m relative to mean sea level, respectively (Mount & Twiss, 2005), and are also part of the Ameriflux Network (Figure 1). Wetland vegetation at both sites consists mainly of tules (*Schoenoplectus acutus*) and cattails (*Typha* spp.), although reeds (*Phragmites* spp.) are also present at Mayberry. The major differences between these two wetlands are the time since restoration (wetland age), past land uses, size, and landscape configuration. Differences in bathymetry during wetland construction led to differences in the fraction of open water versus vegetation at each site. Mayberry wetland was constructed with heterogeneous bathymetry by excavating channels (up to 2 m deep) to provide a mosaic of open water and emergent vegetation. In contrast, West Pond was constructed by evenly excavating the soils of the former agricultural field to create berms for the wetland. The even and shallow bathymetry at West Pond has allowed for a very dense and homogeneous vegetation canopy to develop, with little to no areas of open water. The water table at both wetlands is managed to be above ground level via a system of inlets and outlets. At Mayberry, adjacent river water is piped in occasionally during the dry summer months to compensate for evaporative losses and is conveyed within the wetland system via gravity flow through the conveyor channels. At West Pond, fresh water is piped in continuously from the San Joaquin River and enter the site through an inlet on the southwest corner. Outflows are weirs in the north side of the managed wetlands that are raised to compensate for the accumulation of peat and are designed to collect the surface layer of water only, reducing high flows and minimizing losses from erosion or export (Miller et al., 2008).

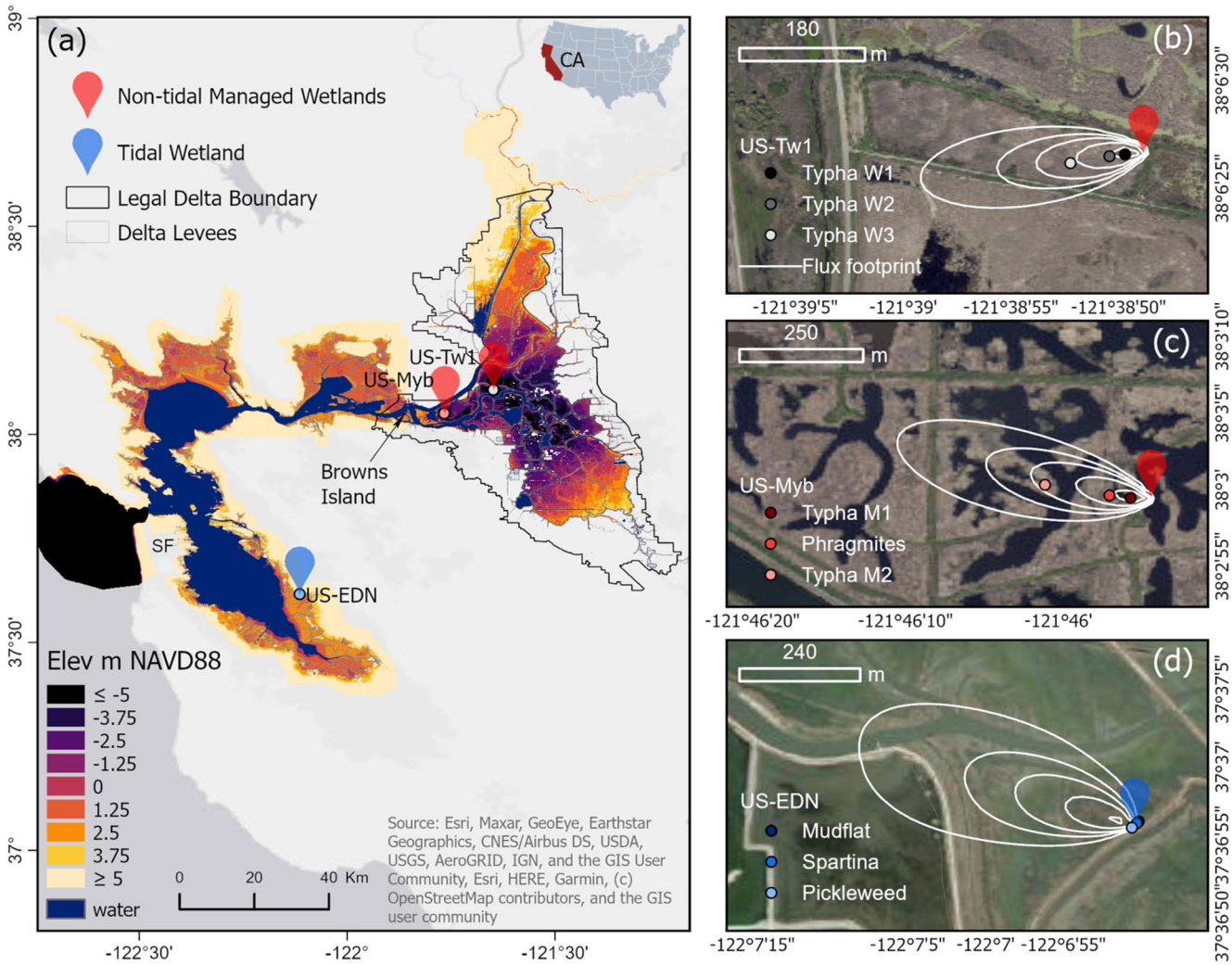

Figure 1. Overview of the San Francisco Bay-Delta with a digital elevation model from Fregoso et al. (2017) (a) and wetland study locations (b–d). Pins represent eddy covariance tower locations and footprint rings correspond, from largest to smallest, to the 90%, 85%, 80%, 70%, and 50% cumulative flux footprints. Solid circles are soil core locations.

2.2. Wetland–Atmosphere Carbon Exchange

Wetland-atmosphere exchange of CO_2 (net ecosystem exchange, NEE) and CH_4 (FCH_4) were quantified using the EC method (Baldocchi et al., 1988) and were accompanied by a suite of supporting meteorological and environmental measurements. Fluxes were calculated from high-frequency (20 Hz) continuous recordings of temperature, water vapor, CO_2, and CH_4 concentrations, along with three-dimensional measurements of wind velocities using open path infrared gas analyzers (LI-7500 and LI-7700, for CO_2 and CH_4, respectively; Li-COR Biosciences, NE, USA) and a 3-D sonic anemometer mounted on a scaffold at each wetland. High-frequency data were integrated to 30 min intervals, and half-hourly fluxes were calculated from the covariance between fluctuations in the vertical wind velocity and concentrations of CO_2 and CH_4 using in-house MATLAB software (Detto et al., 2010; Knox et al., 2015). A detailed description of tower instrumentation and data processing can be found in the Supporting Information of Chamberlain et al. (2018), Eichelmann et al. (2018), and Knox et al. (2018). Briefly, flux corrections and quality control were applied and included high-frequency data despiking, 2-D coordinate rotations, density corrections, and site-specific friction velocity (u*) filtering (Chamberlain et al., 2017; Knox et al., 2015). Fluxes were further filtered for wind directions 290°–240° at West Pond (US-Tw1) to avoid accounting for fluxes from adjacent wetland types. We gap-filled missing fluxes using artificial neural networks (ANNs) as previously

outlined in Knox et al. (2015, 2018). Gap filling relied on model inputs based on season, time of day, net radiation, water, soil and air temperature, water table depth, vapor pressure deficit, friction velocity, and latent heat (Moffat et al., 2007; Papale et al., 2006). The median of the 20 ANN predictions was used to fill missing fluxes, and the variance was used to estimate gap-filling uncertainty.

The net atmospheric C exchange was computed from the integrated annual sum of NEE (g C−CO_2 m^{-2} yr^{-1}, where negative denotes net ecosystem CO_2 uptake) and FCH_4 (g C−CH_4 m^{-2} yr^{-1}) after gap filling and was compared with estimates of organic C accumulation rates (CAR) derived from soil cores and ^{210}Pb and ^{137}Cs radiometric dating. Here, CAR was used as a proxy for the Net Ecosystem Carbon Balance (NECB) (Equation 1).

$$NECB = -NEE + FCH_4 + F_{hydrologic} \quad (1)$$

It should be noted that the sign of NEE generally depends on discipline and is often study-specific. $F_{\text{hydrologic}}$ is the wetland C flux leaving the system via lateral hydrologic export (e.g., in the form of particulate and dissolved organic and inorganic C).

2.3. Soil Organic Carbon Accumulation Rates (CARs)

Three soil cores were taken at each wetland site within the EC flux footprint in 2019 (total $n = 9$ cores). At the tidal wetland (US-EDN), short cores (24–35 cm long, 10 cm inner diameter) were collected by manually inserting PVC tubes into the soil at the three main landcover types present at the wetland: "mudflat," "spartina," and "pickleweed." At the two managed wetlands (US-Tw1 and US-Myb), three cores at each site were collected using a barge-mounted tripod and PVC piston corer (150 cm long and 6.2–10 cm inner diameter) following methods adapted from Sansone et al. (1994). A cutting head and a core catcher were attached to the bottom edge of the PVC tubes to cut through roots and rhizomes, reducing compaction of peat soils and preventing losses when raising the tube from the borehole. Despite efforts to minimize compaction, differences between the core insertion depth and the depth of the retrieved peat were observed and recorded, and compaction corrections to depth layers were applied following Morton and White (1997). Compaction during coring averaged 24% and 17% at West Pond and Mayberry, respectively. Cores were transported to the laboratory, where they were kept refrigerated at 4°C until processing. A soil extruder was used to extract the soils, which were then sliced at 1 to 2 cm-thick intervals for analysis. The different coring methods and slicing thicknesses were chosen according to the soil type, wetland age, peat depth, and expected sedimentation rates. Soil samples were weighed wet and then dried at 60°C until a constant weight was achieved. At the tidal wetland, soil dry bulk density (DBD; g cm^{-3}) was estimated from a 1 cm^3 subsample at each 1 cm-thick slice. At nontidal wetlands, DBD was calculated as the whole slice dry sample mass divided by the core tube volume. The soil mass per unit area (a.k.a. mass depth; g dry soil cm^{-2}), which is not affected by soil compaction (Gifford & Roderick, 2003; Wendt & Hauser, 2013), was estimated at each layer by dividing the dry sample mass by the corer area sampled. CARs were calculated based upon mass per unit area (g cm^{-2}) rather than depth or volume (i.e., DBD) to implicitly correct for artificial and natural compaction and potential uncertainties introduced during manual slicing. For visualization purposes, soil profiles throughout this manuscript were plotted using uncompressed depth.

Soil organic C and total nitrogen contents were measured at 1–3 cm resolution throughout the upper 35 cm and in alternate slices every 5 cm below this depth. Prior to analysis, soil samples were sieved (1 mm) to remove roots and litter before being ground to a fine powder. Subsamples (14–16 mg of tidal wetland soils, and 2–4 mg of nontidal peat soils) were weighed into silver cups, acidified with 1M HCl (tidal soils) and 6% sulfurous acid (nontidal soils), dried at 60°C and analyzed using an elemental analyzer. Stable isotopes of soil organic C ($\delta^{13}C$) were analyzed in nontidal wetland soils using an elemental analyzer–isotope ratio mass spectrometer (Stable Isotope Laboratory, SIL) at the University of California Santa Cruz. Replicate and control samples (acetanilide) were run during C and δ^{13} C analysis. The accuracy and precision of C measurements were ±0.46% and ±0.57%, respectively, and for δ^{13} C, they were ±0.05‰ and ±0.08‰, respectively. Organic matter content (% dry weight) was determined in all soil samples as loss on ignition (LOI) at 550°C for 5 hr (Heiri et al., 2001) and was used to estimate C content of samples where elemental C was not analyzed (i.e., alternate samples in nontidal managed wetland soils) through the C%-LOI% relationship estimated for soils in this study (C% = 0.513 ± 0.007 × LOI% - 1.9 ± 0.4) (Figure S1).

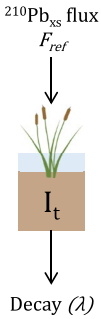

$$\frac{dI}{dt} = F_{ref} - \lambda I; \quad I_t = \frac{F_{\mathbf{ref}}}{\lambda}\left(1 - e^{-\lambda \cdot t}\right) \qquad \text{(Eq. 2)}$$

$$F_{ref} = I_{ref} \cdot \lambda \qquad \text{(Eq. 3)}$$

Figure 2. Box model approach to estimate the $^{210}Pb_{xs}$ inventories accumulated since restoration in nontidal managed wetland soils (*It*). $^{210}Pb_{xs}$ enters the system through atmospheric fallout and leaves through decay. I_t is the $^{210}Pb_{xs}$ inventory accumulated since restoration, F_{ref} is the $^{210}Pb_{xs}$ atmospheric flux in the area, λ is the ^{210}Pb decay constant (0.03108 years^{-1}), and t is the time since restoration.

Specific activities of ^{210}Pb were measured in all cores to assess soil and C accumulation rates since restoration. In tidal wetland soils, total ^{210}Pb and ^{137}Cs were determined using gamma spectrometry through their emission lines at 46.5 and at 661.6 keV, respectively. In managed wetland soils, total ^{210}Pb was determined using alpha spectrometry through the analysis of its granddaughter ^{210}Po after complete sample digestion following Sanchez-Cabeza et al. (1998). The certified reference material IAEA-447 was analyzed alongside soil samples, and the accuracy of the ^{210}Pb(^{210}Po) measurements averaged 96 ± 4%. The specific activities of excess ^{210}Pb ($^{210}Pb_{xs}$) used to obtain the age models were determined as the difference between total ^{210}Pb and ^{226}Ra (supported ^{210}Pb). Specific activities of ^{226}Ra were determined by gamma spectrometry through the measurement of its decay product, ^{214}Pb, at 295 and 352 keV using calibrated geometries in HPGe detectors (CANBERRA, Mod. BE3825, and CANBERRA, Mod. SAGe Well). ^{226}Ra was determined in all sampled depths in tidal wetland soils and in selected depths along managed nontidal wetland soils. In the latter, total ^{210}Pb activities at depth derived by alpha spectrometry and ^{226}Ra specific activities via gamma were within error of one another, confirming the agreement between alpha and gamma methods. Disaggregated soil core data from this manuscript is available at Arias-Ortiz et al. (2021) and Carlin et al. (2021).

Carbon accumulation rates since restoration were estimated by integrating soil organic C stocks down to the restoration depth (in areal mass units; g dry soil cm^{-2}) and dividing by wetland age (t) (i.e., the time elapsed since planting). The depth of restoration was identified using ^{210}Pb age-depth models in tidal wetland soils (US-EDN). Specifically, we applied the Constant Rate of Supply (CRS) (Appleby & Oldfield, 1978) and its Bayesian counterpart, the Plum model (Aquino-López et al., 2018), to date soils. We validated the resulting chronologies independently with the 1963 ^{137}Cs specific activity peak, corresponding to the time of maximum deposition from nuclear atmospheric testing (Robbins & Edgington, 1975).

Regular ^{210}Pb dating models could not be applied in soils from nontidal managed wetlands, which were excavated for restoration purposes. At these sites, we used a box model approach (Figure 2, Equation 2) based on the annual atmospheric flux of $^{210}Pb_{xs}$ estimated for the area (F_{ref} = 36 ± 3 Bq m^{-2} yr^{-1}). The atmospheric flux of $^{210}Pb_{xs}$ was calculated through Equation 3 in Figure 2 from the mean $^{210}Pb_{xs}$ inventory (I_{ref} = 1140 ± 96 Bq m^{-2}) of six dated intact wetland soils in Browns Island (Callaway et al., 2012), which is 10–20 km away from our sites (Figure 1). Direct measurements of $^{210}Pb_{xs}$ atmospheric deposition in artificial collectors in Berkeley, CA, were 32 ± 2 Bq m^{-2} yr^{-1} (Monaghan et al., 1986) and further corroborated our reference $^{210}Pb_{xs}$ flux estimate. The box model was applied to calculate the $^{210}Pb_{xs}$ inventory (I_t) expected to have accumulated since restoration (t) at each site (Equation 2). The restoration depth was then inferred from the soil mass-depth (g cm^{-2}) at which these inventories were met.

Differences in annual NEE, FCH_4, net atmospheric C uptake (−NEE + FCH_4), and C accumulation rates between restored wetland sites were analyzed using an ANOVA and a least significant difference (LSD) means comparison test after confirming normality of their distribution with a Shapiro-Wilk test. All statistics were run using a level of significance of <0.05.

2.4. Wetland Radiative Balance and Radiative Forcing

We estimated the radiative balance (i.e., the radiative state of an ecosystem) for each of the restored wetlands by modeling the fate of atmospheric CO_2 and CH_4 as they are sequestered by, or emitted from, the restored wetlands. We used a modeling approach of sustained CH_4 and CO_2 fluxes as described in Neubauer (2014) at annual time steps. Methane emissions from EC measurement systems and soil organic C accumulation rates were used as input variables. High-frequency NEE fluxes were not used to model CO_2 sequestration since the fate of the potential hydrologic C export remains unknown. Different radiative efficiencies and atmospheric residence times of CO_2 and CH_4 were considered, as well as the oxidation of CH_4 to CO_2 and the atmospheric CO_2 feedbacks with various non-atmospheric reservoirs (Table S1). The CO_2 and CH_4 pools were converted to kg CO_2 and kg CH_4, respectively, before applying radiative efficiency values. The radiative

balance of restored wetlands was modeled for a 500-year period under stable environmental conditions considering (1) the net radiative effect of CH_4 emissions and CO_2 sequestration at a moment in time (instantaneous radiative balance) and (2) the net cumulative effect of CH_4 and CO_2 dynamics integrated over the entire modeled period (cumulative radiative balance). The debate continues about how to best interpret CO_2 equivalent emissions of the shorter-lived CH_4 compared to CO_2 (Allen et al., 2018; Lynch et al., 2020; Neubauer & Megonigal, 2015; Rogelj & Schleussner, 2019). For this reason, we have chosen to model the radiative forcing of CO_2 and CH_4 flux dynamics as described above rather than using a particular standard metric, for example, the Global Warming Potential (GWP) (Myhre et al., 2013) or the Sustained-flux Global Warming Potential (SGWP) (Neubauer & Megonigal, 2015). The wetland switchover time (this is the time needed to switch from a positive to a neutral or negative radiative balance) was determined as the crossover point where net radiative balance reaches zero. This occurs when the warming effect due to CH_4 emissions is overtaken by the cumulative removal (i.e., cooling effect) of CO_2. We run a Monte Carlo simulation ($n = 1{,}000$) to capture the variability in switchover times due to the interannual variability in CH_4 emissions and uncertainty in soil CARs.

To appreciate the effects of wetland restoration on climate, the impact of a restoration action, or "radiative forcing," was considered relative to the baseline condition of greenhouse gas emissions prior to restoration. We used the same modeling approach described above adapted to account for changes in CH_4 and CO_2 instead of the magnitude of these fluxes. The change in the radiative forcing (Δ) caused by marsh restoration was calculated as the difference between the radiative balance of the restored wetland and that of the previous land use (salt pond at US-EDN, pasture at US-Myb, and corn field at US-Tw1). Greenhouse gas emissions and sequestration from crop- and pasturelands in the Delta have been estimated by Hemes et al. (2019) using EC flux systems. Specifically, we used published data from Twitchell corn and Sherman pasture as they are located in the same Delta Islands as our managed wetlands and would have similar soil C stocks and characteristics to pre-restoration land uses. Baseline CO_2 sequestration during salt pond harvesting at the restored tidal marsh was estimated from the age-depth model and soil organic C content accumulated between 1900 and 1970 when salt harvesting was active. A steady decrease in soil C content during and after this period was not observed in soil cores at the tidal wetland, suggesting that changes in soil C content with depth were unrelated to C loss with age. Methane emissions during salt pond operation were considered negligible, which may be a reasonable assumption given the brine conditions (salinity >50) and the low CH_4 emissions observed at salinities >20 (Poffenbarger et al., 2011). In addition, in the absence of available estimates, it is conservative to assume that no CH_4 was emitted from the baseline condition while considering CH_4 emissions from the restoration project.

3. Results

3.1. Wetland-Atmosphere C Balance

Eddy covariance CO_2 and CH_4 flux measurements showed that the three restored wetlands had a net negative atmospheric C balance (denoting C removal from the atmosphere) on an annual basis averaged over 3–9 years (Figure 3). Seasonal variations in CO_2 flux were observed at the three sites. The restored tidal wetland (US-EDN) was net autotrophic nearly year-round (negative NEE), with higher uptake rates observed during the growing season and low net respiration only during the winter months of December and January. Nontidal wetlands with managed hydrology exhibited net CO_2 uptake (negative NEE) during the growing season but net respiration (positive NEE) during the winter months (Figure 3). Cumulative NEE for all years on record was negative at the three sites, averaging -386 ± 28 g C-CO_2 m^{-2} yr^{-1} at the restored tidal wetland, and -334 ± 70 and -357 ± 102 g C-CO_2 m^{-2} yr^{-1} at the young (US-MyB) and old (US-Tw1) managed wetlands, respectively (mean $\pm$ interannual standard error). No significant differences were observed in mean multiyear NEE between sites (ANOVA; $F_{2,17} = 0.06$, $p = 0.94$).

Methane emissions were large in restored wetlands with managed hydrology and peaked 10–15 days after maximum net ecosystem productivity during the growing season. In contrast, negligible CH_4 emissions were observed at the restored tidal wetland during most of the year, with low fluxes between June and September. Annual cumulative emissions of CH_4 were 0.62 ± 0.20 g C-CH_4 m^{-2} yr^{-1} at the tidal restored wetland, which contrasts with cumulative yearly emissions of 44 ± 5 and 37 ± 4 g C-CH_4 m^{-2} yr^{-1} at the young and old nontidal managed wetlands, respectively. Significant differences were observed in mean multiyear

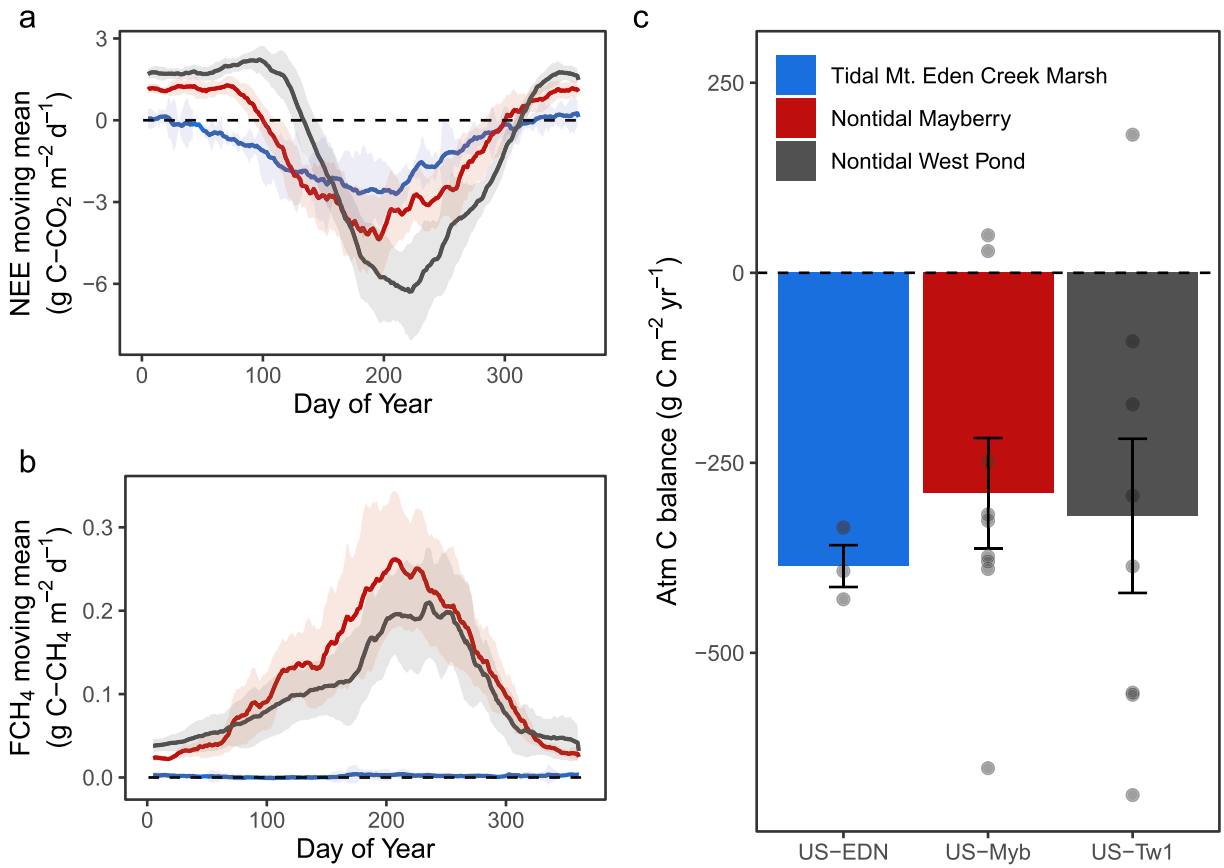

Figure 3. Wetland mean (10 days moving mean) net ecosystem exchange (NEE), methane flux (FCH_4) (a and b) and integrated atmospheric carbon balance ($-NEE + FCH_4$) (c) for all vegetated years on record. Shaded area indicates 95% confidence intervals. Filled circles in panel c indicate net atmospheric C balance for individual years. Entire time-series in Figure S2. All vegetated site-years exclude the first year of restoration at Mayberry before vegetation was established.

FCH_4 between the restored tidal and nontidal managed wetlands (ANOVA; $F_{2,17} = 12.7$, $p < 0.001$), but the means test for multiple comparisons found that FCH_4 was not significantly different between the two nontidal managed wetlands ($p = 0.29$, 95% C.I. = −6.5, 20.2).

The net atmospheric C balance between uptake and emissions (i.e., $-NEE + FCH_4$) was negative at the three restored wetlands and accounted for −386 ± 28, −290 ± 72 and −320 ± 101 g C m^{-2} yr^{-1} at the tidal wetland and young and old managed wetlands, respectively. Although the multiyear net C balance was not significantly different between the sites (ANOVA; $F_{2,17} = 0.18$, $p = 0.83$), large interannual variability was observed at nontidal wetlands with managed hydrology (Figure 3).

3.2. CARs and NECB

Results from soil cores showed that organic carbon content varied with depth and increased from tidal to nontidal managed wetlands and with restoration age (Figure 4). On average, organic C content in the upper ~30 cm of soils in the restored tidal wetland (~20 g cm^{-2}) was 7–10 times lower than that in restored nontidal wetlands with managed hydrology over the same mass depth horizon, which was equivalent to ~45 and ~85 cm at the young and old managed wetlands, respectively. Differences in organic C content across restored wetlands were even more pronounced in surface soils. Surface organic C content in tidal wetland soils ranged between 2.7% and 4.4% and decreased in the upper 5 cm. Below this depth, organic C content fluctuated between surface concentrations and ~1.5%–2%. In restored nontidal wetlands, soil C content ranged between 18% and 40% in the upper ~5 and ~37 cm in the young and old managed wetlands, respectively. Below these depths, organic C content remained constant at 15%–18% and increased to values

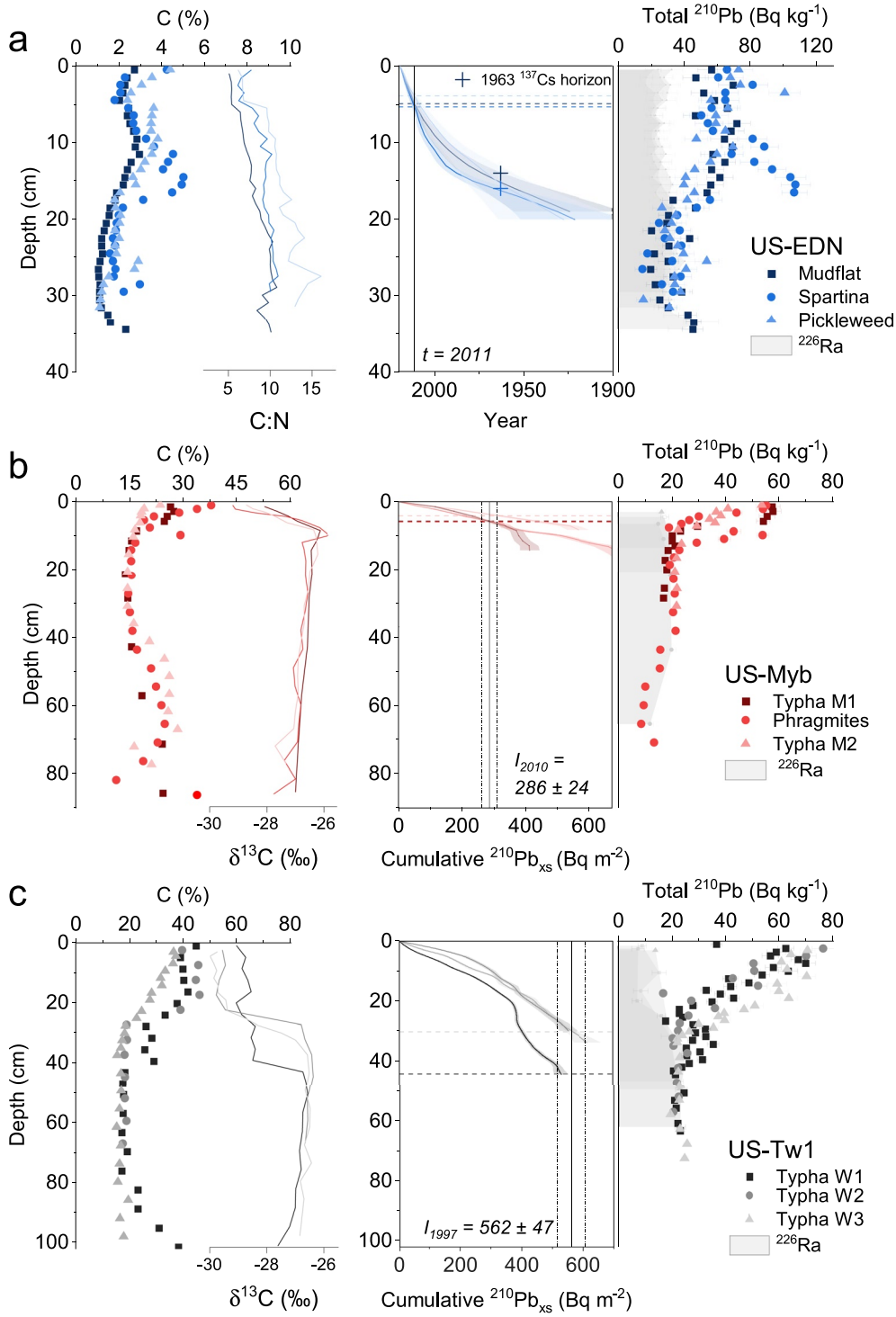

Figure 4. Soil organic carbon, (c) N and δ^{13} C depth profiles (left) and ^{210}Pb results (right) for the soil cores collected in the tidal wetland US-EDN (a) and nontidal wetlands with managed hydrology: US-Myb (b) US-Tw1 (c). Vertical lines indicate the year of restoration *t* (a) or expected $^{210}Pb_{xs}$ inventory accumulated since restoration (I_t) (b), (c). Horizontal lines indicate restoration depth. Note that the scale of the horizontal axis differs between panels. Dry bulk density and ^{137}Cs depth profiles in Figure S3.

Table 2
Mean Sediment and Organic Carbon Accumulation Rates in the Tidal and Nontidal Wetlands With Managed Hydrology Since Restoration

Site id	Years since restoration	Core id	MAR (g cm^{-2} yr^{-1})	SAR (cm yr^{-1})	CAR (g C m^{-2} yr^{-1})
US-EDN	8	Mudflat	0.22 ± 0.05	0.62 ± 0.14	51 ± 12
		Spartina	0.34 ± 0.06	0.65 ± 0.12	85 ± 16
		Pickleweed	0.22 ± 0.05	0.49 ± 0.12	73 ± 17
		Mean SD	0.26 ± 0.08	0.56 ± 0.11	70 ± 19
US-Myb	9	Typha M1	0.08 ± 0.02	0.63 ± 0.07	220 ± 40
		Phragmites	0.16 ± 0.03	0.61 ± 0.05	375 ± 70
		Typha M2	0.125 ± 0.013	0.40 ± 0.03	240 ± 25
		Mean SD	0.12 ± 0.04	0.55 ± 0.13	280 ± 90
US-Tw1	22	Typha W1	0.14 ± 0.04	2.2 ± 0.6	460 ± 140
		Typha W2	0.15 ± 0.05	1.4 ± 0.2	370 ± 120
		Typha W3	0.08 ± 0.04	1.32 ± 0.15	210 ± 100
		Mean SD	0.12 ± 0.05	1.65 ± 0.54	350 ± 150

Note. MAR refers to mass accumulation rate, SAR to soil accretion rate, and CAR to organic carbon accumulation rate. Nontidal wetland SARs were corrected for core compaction thus should be considered as apparent rates.

of 25%–30% below 80 cm. Differences in soil DBD across sites followed the opposite trend than that of organic C (Figure S3).

Excess ^{210}Pb was found in all cores and, despite some variability, it decreased from the surface to below detection at depths between 18 and 20 cm (11 g cm^{-2}) at the tidal wetland, 8–14 cm (4 g cm^{-2}) at the young nontidal wetland, and between 30 and 44 cm (3 g cm^{-2}) at the old managed wetland (Figure 4). Mean mass and organic C accumulation rates since restoration were estimated by integrating soil mass and organic C stocks down to the depth of restoration and dividing by the wetland's age at the time of core collection. The depth of restoration at the tidal wetland (i.e., 2011) was found at 4–5 cm (1.8–2.7 g cm^{-2}) by applying the Plum dating model (Figure 4), which yielded similar results as the CRS model in the upper 15 cm (Figure S4). These chronologies were further validated by the 1963 maximum fallout of ^{137}Cs at 13–15 cm, which presence also excluded the possibility of mixing downcore in 2 of the 3 soil profiles (Figures 4 and S3). Mean organic C accumulation rates at the restored tidal wetland ranged between 51 ± 12 g C m^{-2} yr^{-1} and 85 ± 16 g C m^{-2} yr^{-1} since restoration (Table 2). During salt harvesting (1900–1970), average soil organic C accumulation rates ranged between 14 ± 8 and 27 ± 18 g C m^{-2} yr^{-1}. At the nontidal wetlands with managed hydrology, the depth of restoration was found at ∼5 cm (or 1.10 g cm^{-2}) at the young managed wetland and at 30–44 cm (or 2.4 g cm^{-2}) at the old managed wetland. These depths correspond to the depth at which the $^{210}Pb_{xs}$ inventories reached 286 ± 24 Bq m^{-2} and 562 ± 47 Bq m^{-2}, respectively, which are the $^{210}Pb_{xs}$ inventories expected to have accumulated since restoration (from 2010 to 2019 after correction for decay during the 9-year period, and from 1997 to 2019 after correction for decay during 22-yr, respectively). The depth marking the onset of restoration at the nontidal wetlands with managed hydrology was accompanied by synoptic shifts in C%, DBD, and a decrease of δ^{13} C, further validating ^{210}Pb results. What was identified as the newly accreted material had very low bulk densities (0.23 and 0.08 g cm^{-3} at the young and old wetlands) and lower δ^{13} C signatures (−28.1 ± 0.2 and −29.1 ± 0.1‰), which drastically changed below the restoration horizon to denser soils (0.63 and 0.54 g cm^{-3}) and higher δ^{13} C (−26.7 ± 0.1‰ at both sites) (Figures 4 and S3).

Mass accumulation rates per unit ground area, which consist of the net accumulation of inorganic and organic material, were higher at the restored tidal wetland (0.26 ± 0.08 g cm^{-2} yr^{-1}) than at nontidal wetlands with managed hydrology (0.12 ± 0.05 g cm^{-2} yr^{-1}). When volume was factored in, the highest accretion rates were registered at the old managed wetland and ranged between 1.3 ± 0.2 and 2.2 ± 0.6 cm yr^{-1}. Mean organic C accumulation rates since restoration were similar at the two nontidal wetlands with managed hydrology and averaged 280 ± 90 and 350 ± 150 g C m^{-2} yr^{-1} at the young and old managed wetlands,

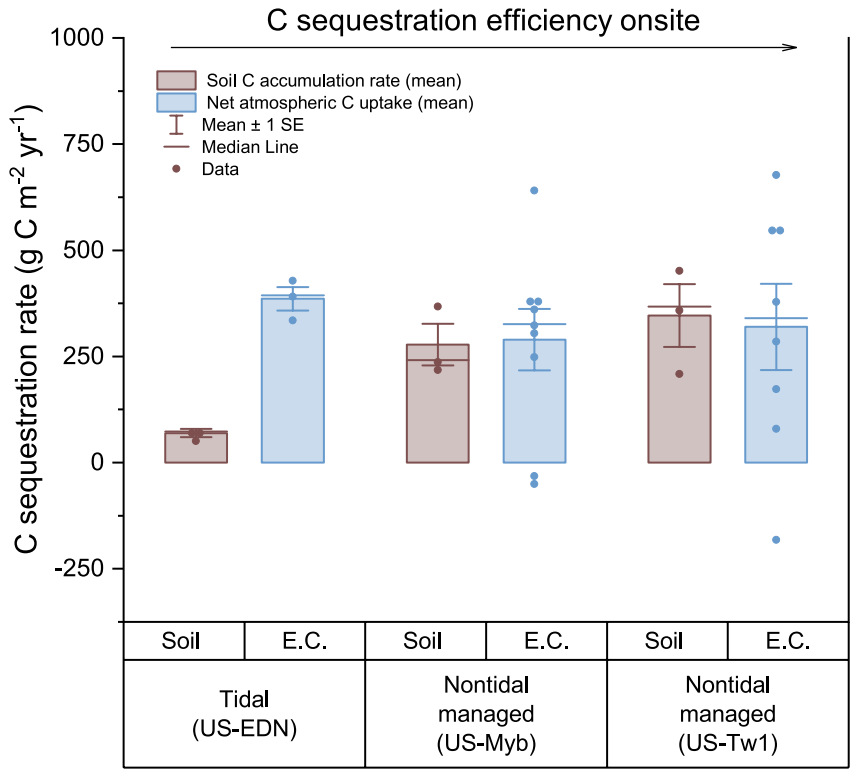

Figure 5. Comparison of carbon sequestration rates as estimated by mean soil carbon accumulation rates since restoration and by eddy covariance net atmospheric carbon uptake (−NEE + FCH_4). Filled circles are estimates from individual soil cores (brown) and from individual eddy covariance vegetated site-years (blue). Organic carbon sequestration rates in soils represent the mean annual estimate since restoration (8 years, 9 years, and 22 years at US-EDN, US-Myb, and US-Tw1, respectively). Eddy covariance carbon sequestration rates represent the multiyear average of individual vegetated site-years (3 years, 9 years, and 8 years at US-EDN, US-Myb, and US-Tw1, respectively).

respectively (Table 2). These rates contrast with the ~5 times lower organic C accumulation of 70 ± 19 g C m^{-2} yr^{-1} observed at the tidal wetland since restoration. Indeed, the estimated soil organic C accumulation rate at the restored tidal wetland was 13%–23% of the net atmospheric C uptake measured by the EC tower. Conversely, no significant differences were observed between net atmospheric C uptake and soil organic C accumulation rates since restoration at nontidal wetlands with managed hydrology (US-Myb: *ANOVA;* $F_{1,10} = 0.008$ $p = 0.94$; US-Tw1: *ANOVA;* $F_{1,9} = 0.02$ $p = 0.88$) (Figure 5)

4. Discussion

4.1. Restored Estuarine Wetlands as Net CO_2 Sinks

The restoration and creation of coastal wetlands have great potential to attract C financing due to the high soil C sequestration rates and large pools of C contained within these systems (Bridgham et al., 2006; Duarte et al., 2013). High rates of wetland C sequestration are a function of high rates of primary productivity, which occur despite the stresses associated with growing in water-saturated and often saline environments. The three restored coastal wetlands in this study were large CO_2 sinks and showed mean annual NEE rates ranging between −386 ± 28 and −334 ± 70 g C−CO_2 m^{-2} yr^{-1}, with no significant differences observed between sites. These rates are in line with those observed in mature fresh and brackish tidal marshes in Louisiana (−337 g C−CO_2 m^{-2} yr^{-1}; Krauss et al., 2016), California (−225 g C−CO_2 m^{-2} yr^{-1}; Knox et al. 2018) or in a salt marsh in Massachusetts (−336 to −256 g C−CO_2 m^{-2} yr^{-1}; Forbrich & Giblin, 2015) and are on the higher end of NEE rates observed in other ecosystems across the world such as in inland peatlands (Bridgham et al., 2006; Webb et al., 2018). The high net ecosystem productivity of the restored wetlands in the San Francisco Bay-Delta is driven by its long growing season, warm air temperatures, large macrophyte vegetation (~3 m tall in nontidal wetlands), and cold water temperatures and inundation that lower annual

ecosystem respiration (Barr et al., 2013; Eichelmann et al., 2018; Guo et al., 2009; Xie et al., 2014). While estuarine wetlands, including our sites, are typically net sinks of atmospheric CO_2, nontidal wetlands with managed hydrology exhibited large interannual variability.

Succession and disturbance have been identified as the causes of variability in previous studies (Chamberlain et al., 2020; Hemes et al., 2019). Insect outbreaks and a drought-induced salinization event reduced CO_2 uptake at the young nontidal managed wetland (US-Myb) to near neutrality during 2013 and 2016, and water table fluctuations caused the largest year-to-year variability at the old nontidal managed wetland (US-Tw1). In the latter, a 6-month period of water tables below the surface spanning halfway into the growing season caused the wetland to become a net CO_2 source during 2019, resulting in between-year variation reaching 480 g C-CO_2 m^{-2} yr^{-1} (Figure S2). Methane emissions are inherently linked to plant productivity (Bridgham et al., 2013); thus, reductions in NEE due to disturbance were often accompanied by reductions in FCH_4 (Figure S2) (Chamberlain et al., 2020; Sturtevant et al., 2016). Unintended short-term water drawdowns have become more frequent in recent years, influencing FCH_4 on multiple time scales and seemingly causing an overall decreasing trend at the young and old managed wetlands (Figure S2) (Valach et al., 2021). This trend contrasts with those observed at other restored nontidal wetlands in the Delta (Valach et al., 2021), suggesting that ongoing site-specific factors might be driving FCH_4 variability. The shorter record of greenhouse gas exchange at the restored tidal wetland complicates assessing interannual variability, however, the 3 years of NEE recorded at this site are similar (average: −386, range of 95 g C−CO_2 m^{-2} yr^{-1}). Large interannual variability in NEE has been observed in other tidal wetlands undergoing disturbance, but minimal data exists on FCH_4. A tidal mesohaline marsh in Louisiana affected by salinization and submergence was observed to be a net CO_2 source, emitting 171 g C-CO_2 m^{-2} yr^{-1} (Krauss et al., 2016), and an urban tidal marsh in the Hudson-Raritan estuary affected by invasive species showed a 4-fold difference in NEE (from −310 g C-CO_2 m^{-2} yr^{-1} to 984 g C-CO_2 m^{-2} yr^{-1}; Schäfer et al., 2014), highlighting the potential for large interannual variability also in tidal wetland NEE. Studies to attribute cause and effects of year-to-year variability need decades of data (Chu et al., 2017). Such long-term studies are critical if wetland restoration is to be successful, permanent, and an effective tool to mitigate climate change.

4.2. Contrasting Soil and Carbon Accumulation at Tidal and Nontidal Wetlands

^{210}Pb dating and analysis of organic C in soil cores indicated that most or part of the C fixed from the atmosphere was accrued in soils since restoration at nontidal managed and tidal wetlands, respectively. All restored sites in this study were at least a decade old (Table 1), providing enough time for vegetation growth and litter accumulation cycles to establish (Valach et al., 2021) as well as for the successive burial of yearly mineral and organic matter cohorts, leading to observable changes in soil properties. Soil C accumulation rates in this study were estimated since restoration. Therefore, they should be considered short-term rates, given that the process of soil development and peat formation encompasses centuries to millennia (Drexler, 2011; Drexler, Fontaine, & Brown, 2009).

Soil organic C accumulation rates estimated since restoration averaged 70 ± 20 g C m^{-2} yr^{-1} at the tidal wetland (US-EDN), in good agreement with the average C accumulation rate of 79 g C m^{-2} yr^{-1} estimated across tidal wetlands in the San Francisco Bay-Estuary based on ^{210}Pb dating (Callaway et al., 2012). The organic C accumulation at the restored tidal wetland constituted a small fraction (~3%) of the bulk accumulation, dominated by the mineral fraction (Figure 4). This explains the two times higher mass accumulation rate observed at the restored tidal wetland than those measured at nontidal wetlands with managed hydrology (tidal: 0.26 ± 0.08 g cm^{-2} yr^{-1} and nontidal: 0.12 ± 0.05 g cm^{-2} yr^{-1}). In the latter, biomass accumulation from emergent vegetation was primarily responsible for the observed soil accretion and organic C accumulation rates. The newly accreted material had low DBD (0.08–0.23 g cm^{-3}) and high organic C content (18%–44%), resembling historic unoxidized peat soils in the Delta (0.19 g cm^{-3} and 30% C; Drexler, Fontaine, and Brown [2009]), which were also preserved in our cores below 80 cm depth (Figure 4). Low values of δ^{13} C observed in the newly accreted material, typical of emergent vascular plants such as cattails (~−31 to −22‰) (Cloern et al., 2002), further reflected the critical contribution of autochthonous biomass accumulation to soil accretion and C sequestration in nontidal managed wetlands. Soil accretion rates ranged from 0.56 ± 0.11 cm yr^{-1} at the tidal and young managed wetland to 1.65 ± 0.54 cm yr^{-1} at the old nontidal wetland with managed hydrology. The 3-fold difference in soil accretion rates observed between restored

wetland sites can be explained by the mineral versus organic nature of the newly accumulated soils and the effect of shallow permanent flooding on enhancing vertical accretion. Previous studies have shown that the organic fraction produces nearly all the volume of the soil (Craft et al., 1993; Redfield, 1972) and that vertical accretion at sites characterized by organic root-bound mass substrates, like the nontidal wetlands in this study, is strongly affected by hydrologic factors and substrate buoyancy (Ewing & Vepraskas, 2006; Miller et al., 2008). The latter is evidenced by the difference in accretion rates between the old and young nontidal managed wetlands, which despite having similar ecosystem productivity and soil characteristics, standing water at the young nontidal wetland is limited to channels as opposed to the old wetland, which is homogeneously flooded to depths of about 25 cm.

4.3. Wetland Carbon Flux Stoichiometry

Nontidal wetlands with managed hydrology showed the largest soil C sequestration efficiency on-site, as the mean multiyear net atmospheric C uptake was equivalent to the mean organic C accumulation rate in soils (Figure 5). The managed nontidal wetland design with long water residence times and limited erosion or export (Miller et al., 2008) resulted in efficient trapping of autochthonous C while limiting the sources of C loss to decomposition *in situ*, thus explaining the excellent agreement between soil organic C accumulation rates since restoration and EC atmospheric C flux measurements. At the restored tidal wetland, soil organic C accumulation rates since restoration were 4–5 times lower than those at the nontidal managed wetlands, despite no significant differences in net ecosystem C exchange (NEE) were observed between sites. Indeed, mean organic C accumulation rates since restoration accounted for only 13%–23% of the fixed atmospheric C at the tidal wetland site, suggesting that lateral hydrologic export is reducing on-site C sequestration.

The difference between the estimated net atmospheric C uptake ($-NEE + FCH_4$) and the mean soil organic C accumulation rate since restoration at the tidal wetland would suggest a first-order estimate of lateral C export of 320 ± 30 g C m^{-2} yr^{-1}. This is considerably larger than estimates of 70–100 g C m^{-2} yr^{-1} reported by Forbrich et al. (2018) and Bogard et al. (2020) in high marsh settings characterized by limited drainage and flooding frequency, but align with estimates of C export from other sites experiencing semidiurnal flooding (from 414 to ~1,500 g C m^{-2} yr^{-1}; Chu et al., 2018; Maher et al., 2013, 2018; Wang et al., 2016). The hydrologic C export estimated by Forbrich et al. (2018) and Bogard et al. (2020) accounted for 40%–50% of the marsh NEE and was similar to, or lower than, the marsh soil C accumulation rate. In contrast, the lateral inorganic C export estimated by Wang et al. (2016) and Chu et al. (2018) from an intertidal polyhaline marsh was 4–9 times larger than the estimated C burial rate (120 ± 50 g C m^{-2} yr^{-1}, Gonneea et al., 2019) similar to Maher et al. (2018), where the total lateral C flux from a mangrove ecosystem was 10 times the soil C burial rate. These flux stoichiometries are comparable to those observed at US-EDN, where the estimated lateral C export is between 4 to 7 times larger than the observed soil C accumulation rate and accounts for ~80%–90% of its net atmospheric C uptake. Although our estimate is a first-order estimate of the average lateral C export since restoration, it is in line with global estimates of tidal wetland C budgets, which suggest that 80 ± 7% of the net C uptake from the atmosphere is balanced by net lateral export to adjacent water bodies, with only 20 ± 7% buried in soils or sediments (Najjar et al., 2018).

An increasing number of studies identify dissolved inorganic C to be the dominant form of C exported via tidal exchange in tidal marshes and mangroves (Bogard et al., 2020; Cabral et al., 2021; Maher et al., 2018; Santos et al., 2019; Taillardat et al., 2018). Preliminary lateral C flux data at US-EDN suggest that the bulk of the C export is as dissolved inorganic C, mainly in bicarbonate form with much smaller fractions as dissolved CO_2 and carbonate (pers. comm. Oikawa). Further research is needed to constrain the fate of the hydrologic C export, however, C exported as carbonate and bicarbonate (i.e., as carbonate alkalinity) is more likely to be stored in the ocean compared to C exported as CO_2, which will return to the atmosphere on short time scales (Santos et al., 2021).

4.4. Influence of Wetland Restoration on Climate

When a wetland is degraded and drained, greenhouse gas fluxes often shift toward increased oxidation of soil C to atmospheric CO_2 and reductions in rates of CH_4 emissions. Conversely, when wetlands are reflooded, or the hydrology is restored and vegetation re-established, soil organic C accumulates, and greenhouse

gas fluxes may change direction. Evidence for enhanced CO_2 emissions from degraded agricultural peat soils and the potential for restored wetlands to sequester C is widespread in the Sacramento-San Joaquin Delta and elsewhere (Evans et al., 2021; Hatala et al., 2012; Hemes et al., 2019). Hemes et al. (2019) showed that degraded agricultural peat soils were consistently neutral to net C sources, losing C to the atmosphere mostly in the form of ecosystem CO_2 respiration, and that restored wetlands, on the other hand, were consistently neutral to negative C emitters, with unintended CH_4 emissions. Restoring drained landscapes back to flooded conditions has been shown to inhibit soil C oxidation; however this often comes at the cost of increased CH_4 emissions, particularly in fresh and oligohaline systems (Hemes et al., 2018; Poffenbarger et al., 2011). Permanent freshwater flooding combined with warm air temperatures, C-rich soils, and a long growing season results in large CH_4 emissions as observed at the nontidal wetlands with managed hydrology in this study (Figure 3), which record some of the highest CH_4 fluxes measured across similar wetlands around the world (Bridgham et al., 2006; Hemes et al., 2018) and contrast with the >40-fold lower CH_4 fluxes observed at the restored tidal wetland, growing in the same climate and region. The euhaline conditions at the tidal wetland play an important role in the very low CH_4 fluxes observed at this site, however, low CH_4 fluxes (~1.1 g CH_4 m^{-2} yr^{-1}) and high CO_2 sequestration to CH_4 emission ratio (245:1) have also been observed in an oligohaline tidal wetland in the Bay-Delta (US-Srr) (Callaway et al., 2012; Windham-Myers et al., 2020), suggesting that incoming and receding tides may also play a role modulating CH_4 emissions, for example through the replenishment of terminal electron acceptors that suppress methanogenesis, such as sulphate, nitrate, and oxygen (Emery & Fulweiler, 2017; Kroeger et al., 2017).

The ratio of CO_2 sequestration to CH_4 emissions and the C fluxes from the previous land-use determine how long it takes for a newly restored wetland to have a net cooling effect (negative radiative forcing) (Neubauer, 2021). Because a kilogram of CH_4 in the atmosphere has about 94.4 times the warming potential of a kg of CO_2 at time 0 (i.e., the ratio of CH_4 and CO_2 radiative efficiencies as modeled in Neubauer, 2014 and here), high C sequestration rates may not imply immediate climate mitigation benefits if the sequestration to emissions ratio does not exceed the figure of 94.4. Examples are the restored wetlands with managed hydrology in this study, that despite having a high C sequestration efficiency on-site, exhibited sequestration to emission ratios that were on average 17:1 and 24:1 at the young (US-Myb) and old (US-Tw1) managed wetlands, respectively, as opposed to the restored tidal wetland with a ratio of 310:1 (kg/kg). At sequestration to emission ratios of 17 and 24, ecosystem CH_4 emissions fully offset CO_2 sequestration for the first 190 years (range 90–390 years) and 108 years (range 50–260 years), respectively, if the instantaneous radiative balance approach is used (Figure 6a). If the cumulative radiative balance approach is considered instead, the switchover time would occur 2 times later (Figure 6b).

Counterintuitively, the effect of a wetland restoration action on climate is not measured by the wetland's radiative balance but by the change in the net radiative balance of the system relative to the previous land use condition (i.e., its radiative forcing). The switchover time can be substantially reduced when considering the radiative forcing effect of the different restoration actions (i.e., change in the radiative balance of the system relative to the previous land use). Despite a large range of uncertainty due to interannual variability in annual CH_4 fluxes and CO_2 sequestration, and in the emission burden of the previous land use condition, our model suggested that the restoration of the tidal wetland from a prior salt pond contributed to a net cooling effect (negative Δ radiative forcing), with low amounts of cooling during the firsts years that increased with time with the accumulation of organic C in soils under stable environmental conditions (Figures 6c–6f). In contrast, restoration of nontidal managed wetlands from pasture and agricultural lands led to an initial net warming effect (positive Δ radiative forcing) lasting 4.5 $\pm$ 3.5 and 2.1 $\pm$ 2.0 decades if the instantaneous radiative forcing approach was used, or 8.1 $\pm$ 4.3 and 3.3 $\pm$ 3.0 decades at US-Myb and US-Tw1, respectively, if the cumulative radiative forcing approach was considered (Figures 6c–6f). Shortly after the crossover point from warming to cooling, the net cooling effect provided by the cumulative C sequestration of restored nontidal wetlands with managed hydrology exceeded that provided by the restored tidal wetland, assuming effective management is sustained over time and that the hydrologic C export from the tidal wetland is consumed offshore.

Available short-term estimates, as well as global summaries of hydrologic C export (Santos et al., 2021), suggest that the hydrological C transport is followed by ocean storage if exported as alkalinity. Although more research is required to quantify alkalinity export at the restored tidal wetland, this would only increase its C

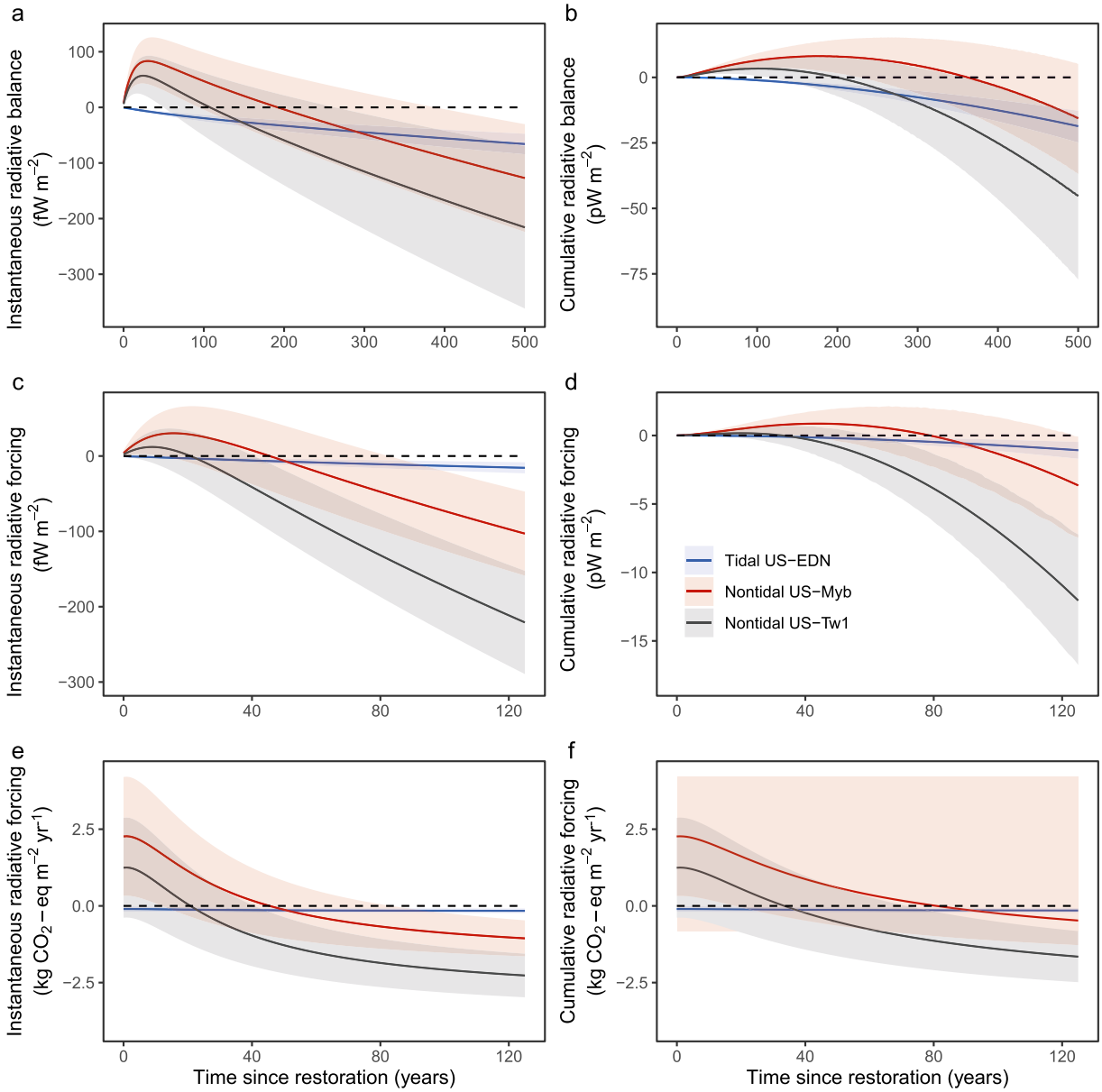

Figure 6. Radiative balance and net radiative forcing of restored wetlands modeled over a 125 to 500-year period. Instantaneous and cumulative wetland's radiative balance (a and b), change in the instantaneous and cumulative radiative forcing following wetland restoration (c and d), and net CO_2-equivalent greenhouse gas fluxes (e and f). The Δ radiative forcing is calculated as the difference between the radiative balance of the restored wetlands and that of the previous land use (salt pond at US-EDN, pasture at US-Myb, and corn field at US-Tw1). Net greenhouse gas fluxes were converted to CO_2-equivalents as the product of the gas flux and the ratio of the cumulative radiative efficiencies of a kg of CH_4 and CO_2 over time, after accounting for the indirect forcings of CH_4 (Neubauer, 2021). The shaded area represents 95% confidence in switchover times. $fW = 10^{-15}$ W, $pW = 10^{-12}$ W.

sequestration capacity, making it an even more potent greenhouse gas sink than what was modeled here. In line with this, prior salt ponds may have had higher CH_4 fluxes than those assumed in the model. This could be related to their nontidal nature and the presence of methanogenic pathways in hypersaline systems (e.g., methylotrophic methanogenesis) that do not necessarily compete with sulphate-reducing bacteria (Kelley et al., 2015; Zhou et al., 2021). If former salt ponds were net CH_4 emitters, this would only increase the added carbon and climate benefits associated with tidal marsh restoration, not only by increasing soil carbon accumulation but also by reducing CH_4 emissions.

This study's dynamic instantaneous and cumulative modeling approaches are similar to those used to model the temporal variations in the GWP and SGWP values, respectively. However, the use of these metrics as a

policy, regulatory, management, or research tool results in a static approach to the climatic role of wetland restoration. Their use often requires the choice of a time horizon (e.g., 20, 100, 500 years) for the conversion of CH_4 fluxes to CO_2-equivalents. For example, Verified Carbon Standard (VCS) guidelines, like other carbon registry standards, specify the use of the GWP metric to convert units of CH_4 emissions to CO_2 equivalents using a 100-year time scale (Needelman et al., 2018). Using this approach, land use conversions to restored wetlands in this study would have resulted in emissions reductions and biogeochemical cooling regardless of the wetland type or tidal influence. Likewise, similar results would have been obtained by applying the SGWP over a 100 years timescale; the magnitude of the reductions would have been smaller, but the direction the same (Figure S5). Dynamic modeling approaches such as those used in this study and others (Hemes et al., 2019; Neubauer, 2014; Neubauer & Megonigal, 2015; Neubauer & Verhoeven, 2019) allow for a more detailed assessment of the climatic role of a restored ecosystem over its lifetime. The modeling of the switchover time, as well as the fate of CH_4 and CO_2 as they are emitted from or sequestered by wetlands in this study, is necessary for the realization of the early warming effect of nontidal marsh restoration, and the immediate cooling provided by tidal wetland restoration. These insights are masked if GWP or SGWP metrics are used. At the same time, the static metrics do not allow assessing how overall wetland radiative forcing changes in response to disturbance or biogeochemistry-driven changes in rates of greenhouse gas production and sequestration. Thus, we suggest that dynamic radiative models might be preferable when determining C credits for marsh restoration projects where CH_4 emissions are expected.

4.5. Future Projections

Our projections of the future climatic impact of wetland restoration are limited by uncertainties around wetland responses to changes in climate. Climate change is one of the greatest challenges for coastal and estuarine wetland restoration projects (Callaway et al., 2011). It affects coastal wetlands directly, primarily through changes in the rate of sea-level rise and, second, through salinization. Average rates of sea-level rise between 2030 and 2100 in the San Francisco Bay are predicted to range between 0.4 ± 0.2 and 1.1 ± 0.3 cm yr^{-1} under a 66% probability (OPC, 2018). These rates are within the range of soil accretion estimated in all restored wetlands in this study. However, the sizeable differences in initial surface elevation among sites make nontidal managed wetlands in subsided islands (>3 m below mean sea level) particularly at risk of collapse. Estimated rates of soil accretion observed at nontidal managed wetlands may not be enough to reach mean sea-level before a high risk of levee failure and flooding (Buchanan & Lionberger, 2007). However, their restoration contributes to gains in surface elevation that reduce the trajectory of increasing hydraulic pressures on levees and seepage onto islands while it breaks the unsustainable subsidence cycle from drainage and peat oxidation. With improved management and consistent, permanent flooding, Miller et al. (2008) showed that higher elevation gains (7–9 cm yr^{-1}) are possible. Low water table depths at both nontidal wetlands likely affected soil accretion rates estimated in this study, particularly at the old managed wetland (US-Tw1), dry during a good portion of 2019 and during soil core sampling. Water tables below the surface result in a loss of buoyancy of these marshes and contribute to desiccation and compaction, impacting vertical accretion rates. This serves to highlight the importance of permanently keeping nontidal managed wetlands flooded, not only to avoid soil oxidation and CO_2 emissions but also to sustain high accretion rates in the long term.

Nontidal freshwater and oligohaline wetlands with managed hydrology might also experience salinization associated with periods of drought and saltwater intrusion (Chamberlain et al., 2020). Salinization, often in tandem with low water levels at impounded marshes, can inhibit rates of both photosynthesis and methanogenesis (Glenn et al., 1995; Poffenbarger et al., 2011; Watson & Byrne, 2009), however, whether the reduction in CH_4 production outweighs the decrease in net carbon uptake is uncertain. Reductions in CH_4 emissions might not have a favorable impact on the radiative balance of the system if accompanied by reductions in net productivity. During the peak of a drought-induced salinization event at the young nontidal wetland in this study (US-Myb), reductions in NEE vastly exceeded those of CH_4 (Chamberlain et al., 2020), bringing the CO_2 to CH_4 ratio down to 1 (1 kg CO_2 sequestered per 1 kg CH_4 emitted), thereby causing an increase of the overall radiative balance of the ecosystem. Neubauer (2013) found similar results in a tidal freshwater marsh experiencing saltwater intrusion. The CO_2 to CH_4 ratio decreased from ~19 to 17, causing an overall net warming due to the larger positive radiative forcing from NEE reductions than the negative radiative forcing from drops in CH_4. The response of wetland-atmosphere greenhouse gas exchange to salinization is complex. It will vary depending on the degree of salinization, whether it occurs gradually or in pulsed

events, concurrent changes in hydrology and inundation time, and variations in primary production and ecosystem respiration due to plant community changes, nutrient loading, and meteorological drivers.

In tidal wetlands that can keep pace with accelerating rates of sea-level rise, a rise in sea level could trigger an increase of soil C accretion through enhanced biomass production (Kirwan & Megonigal, 2013; Morris et al., 2002). For example, the restored tidal wetland in this study would survive predicted sea-level rise under a low (0.4 cm yr^{-1}) scenario as simulated by the MEM model (Morris et al., 2002), which projects change in tidal marsh surface elevation with sea-level rise (Table S2) (Figure S6). Therefore, the restored tidal wetland would likely continue to provide a net biogeochemical cooling effect over the next 100 years assuming no changes in CH_4 emissions given the already euhaline (30–40) conditions. However, at high rates of relative sea-level rise (1.10 cm yr^{-1}), the soil organic C accumulation would be adjusted downwards, reducing the wetland's accrual of greenhouse gas benefits (Figure S6). The marsh could potentially collapse toward the end of the century leading to a halt in its C sequestration and the many other ecosystem services. There is a lot of uncertainty about the long-term trajectory of the relationship between C sequestration and emissions in restored or created wetlands under a changing environment. Long-term studies are critical to capture interannual variability in C fluxes driven by succession, disturbance, and climate changes, as well as to more explicitly predict the evolution of the CO_2:CH_4 ratio in future works. The incorporation of climate change modeling into wetland management, restoration and creation will be critical to effectively promote ecosystem resilience, sustained C sequestration, and maintenance of ecosystem services.

5. Conclusions

Combining the EC technique with the more commonly applied greenhouse gas accounting procedures such as soil C stock change provides a comprehensive analysis of C mitigation benefits through the restoration and creation of tidal and nontidal wetlands. It allows quantifying C sequestration and estimation of CH_4 emissions. At the same time, it provides a rough estimate of C export to adjacent areas through hydrologic exchange, which are all essential elements for successful wetland C mitigation projects. Additionally, this combined approach allows understanding the mechanisms by which C is stored or released and informs modeling about how C fluxes may respond to management, disturbance, and climate change. While Blue Carbon projects related to wetland restoration often assume that soil organic C storage results in an immediate climate cooling service, our analyses indicate that this assumption might be inappropriate except, perhaps, in saline environments where wetlands tend to have lower CH_4 emissions. Merits and differences exist in the restoration of nontidal and tidal wetlands in terms of climate change mitigation and adaptation. Restored nontidal wetlands with managed hydrology might be the most efficient at burying C on-site due to their design that minimizes C loss through export, in contrast to restored tidal wetlands. However, the nontidal condition may also favor CH_4 emissions, which in our study incurred a greenhouse gas debt in nontidal wetlands that was only neutralized by its efficient C sequestration after 2 to 4 decades, or 3 to 8 decades on average under stable conditions, depending on the modeling approach used. The restored tidal wetland, yet losing a large fraction of its net atmospheric C uptake through hydrologic export, showed a larger CO_2-sequestration to CH_4-emission ratio. The fact that this was also observed in a tidal oligohaline wetland in the same region may suggest that tidal wetland restoration, when possible, could be a better strategy to achieve climate mitigation benefits in the short and mid-term (≤100 years). In contrast to the climate mitigation service, other economically and valuable wetland services such as soil accretion, or the stopping of surface subsidence caused by drainage, become established right from the start of wetland restoration. Protection for sea-level rise is, in many instances, ranked first in importance and immediacy, followed by CO_2 sequestration and the reduction of the Earth's energy budget. Therefore, services such as soil accretion are relevant in the face of climate change and should motivate on itself restoration projects.

Data Availability Statement

EC data are available on the Ameriflux website: US-EDN (https://doi.org/10.17190/AMF/1543381), US-Myb (https://doi.org/10.17190/AMF/1246139) and US-Tw1 (https://doi.org/10.17190/AMF/1246147). Soil core datasets are available through the Smithsonian's Figshare data repository: Mount Eden Creek Marsh

soils (http://doi.org/10.25573/serc.16416684); Mayberry and West Pond soils (http://doi.org/10.25573/serc.15127743).

Acknowledgments
This work was funded by the California Department of Water Resources (DWR) through a contract from the California Department of Fish and Wildlife, the United States Department of Agriculture McIntire Stennis Capacity Grant to the California Agriculture Experiment Station, the Delta Stewardship Council (agreement #18200) and the California State University Council on Ocean Affairs, Science and Technology (CSU COAST). AA-O was supported by the NOAA C&GC Postdoctoral Fellowship Program administered by UCAR -CPAESS (#NA18NWS4620043B). Funding was provided to P.M. through an Australian Research Council LIEF Project (LE170100219). This work is contributing to the ICTA "Unit of Excellence" (CEX2019-000940-M). The IAEA is grateful for the support provided to its Environment Laboratories by the Government of the Principality of Monaco. The authors acknowledge the work of all Berkeley Biometeorology Lab and Oikawa Lab members who helped maintain towers and collected and processed data over the lifetime of these sites. Thanks to Camilo Rey, Robert Shortt, and Alex Valach, who helped collect soil cores in the Delta. We also thank the Paytan Biogeochemistry Lab for assisting in laboratory analyses and Theresa Duncan and Mathew Kirby for their help in analyzing the tidal marsh sediment samples.

References

Allen, M. R., Shine, K. P., Fuglestvedt, J. S., Millar, R. J., Cain, M., Frame, D. J., & Macey, A. H. (2018). A solution to the misrepresentations of CO_2-equivalent emissions of short-lived climate pollutants under ambitious mitigation. *NPJ Climate and Atmospheric Science*, *1*(1), 1–8. https://doi.org/10.1038/s41612-018-0026-8

Appleby, P. G., & Oldfield, F. (1978). The calculation of lead-210 dates assuming a constant rate of supply of unsupported 210Pb to the sediment. *CATENA*, *5*(1), 1–8. https://doi.org/10.1016/S0341-8162(78)80002-2

Aquino-López, M. A., Blaauw, M., Christen, J. A., & Sanderson, N. K. (2018). Bayesian Analysis of 210 Pb Dating. *Journal of Agricultural, Biological, and Environmental Statistics*, *23*(3), 317–333. https://doi.org/10.1007/s13253-018-0328-7

Arias-Ortiz, A., Masqué, P., Paytan, A., & Baldocchi, D. D. (2021). *Dataset: Tidal and nontidal marsh restoration: A trade-off between carbon sequestration, methane emissions, and soil accretion*. Smithsonian Environmental Research Center. https://doi.org/10.25573/serc.15127743

Baldocchi, D. D. (2020). How eddy covariance flux measurements have contributed to our understanding of Global Change Biology. *Global Change Biology*, *26*(1), 242–260. https://doi.org/10.1111/gcb.14807

Baldocchi, D. D., Hicks, B. B., & Meyers, T. P. (1988). Measuring biosphere-atmosphere exchanges of biologically related gases with micrometeorological methods. *Ecology*, *69*(5), 1331–1340. https://doi.org/10.2307/1941631

Barr, J. G., Engel, V., Fuentes, J. D., Fuller, D. O., & Kwon, H. (2013). Modeling light use efficiency in a subtropical mangrove forest equipped with CO_2 eddy covariance. *Biogeosciences*, *10*(3), 2145–2158. https://doi.org/10.5194/bg-10-2145-2013

Bogard, M. J., Bergamaschi, B. A., Butman, D. E., Anderson, F., Knox, S. H., & Windham-Myers, L. (2020). Hydrologic export is a major component of coastal wetland carbon budgets. *Global Biogeochemical Cycles*, *34*(8), 1–14. https://doi.org/10.1029/2019GB006430

Bridgham, S. D., Cadillo-Quiroz, H., Keller, J. K., & Zhuang, Q. (2013). Methane emissions from wetlands: Biogeochemical, microbial, and modeling perspectives from local to global scales. *Global Change Biology*, *19*(5), 1325–1346. https://doi.org/10.1111/gcb.12131

Bridgham, S. D., Megonigal, J. P., Keller, J. K., Bliss, N. B., & Trettin, C. (2006). The carbon balance of North American wetlands. *Wetlands*, *26*(4), 889–916. https://doi.org/10.1672/0277-5212(2006)26[889:TCBONA]2.0.CO;2

Buchanan, P. A., & Lionberger, M. (2007). *Summary of Suspended-Sediment Concentration Data, San Francisco Bay, California, Water Year 2005*. U.S. Geological Survey Data Series.

Cabral, A., Dittmar, T., Call, M., Scholten, J., de Rezende, C. E., Asp, N., et al. (2021). Carbon and alkalinity outwelling across the groundwater-creek-shelf continuum off Amazonian mangroves. *Limnology and Oceanography Letters*. https://doi.org/10.1002/lol2.10210

Callaway, J. C., Borgnis, E. L., Turner, R. E., & Milan, C. S. (2012). Carbon sequestration and sediment accretion in San Francisco bay tidal wetlands. *Estuaries and Coasts*, *35*(5), 1163–1181. https://doi.org/10.1007/s12237-012-9508-9

Callaway, J. C., Parker, V. T., Vasey, M. C., Schile, L. M., & Herbert, E. R. (2011). San Francisco estuary and watershed science tidal wetland restoration in san Francisco bay: History and current issues. *San Francisco Estuary and Watershed Science*, *9*(3).

Carlin, J., Oikawa, P. Y., Arias-Ortiz, A., Kanneg, S., Duncan, T., & Beener, K. (2021). *Dataset: Sedimentary organic carbon measurements in a restored coastal wetland in San Francisco Bay, CA, USA*. Smithsonian Environmental Research Center. https://doi.org/10.25573/serc.16416684

CDFW. (2020). *Wetlands restoration for greenhouse gas reduction Program*. Retrieved from https://wildlife.ca.gov/Conservation/Watersheds/Greenhouse-Gas-Reduction

Chamberlain, S. D., Anthony, T. L., Silver, W. L., Eichelmann, E., Hemes, K. S., Oikawa, P. Y., et al. (2018). Soil properties and sediment accretion modulate methane fluxes from restored wetlands. *Global Change Biology*, *24*(9), 4107–4121. https://doi.org/10.1111/gcb.14124

Chamberlain, S. D., Hemes, K. S., Eichelmann, E., Szutu, D. J., Verfaillie, J. G., & Baldocchi, D. D. (2020). Effect of drought-induced salinization on wetland methane emissions, gross ecosystem productivity, and their interactions. *Ecosystems*, *23*(3), 675–688. https://doi.org/10.1007/s10021-019-00430-5

Chamberlain, S. D., Verfaillie, J., Eichelmann, E., Hemes, K. S., & Baldocchi, D. D. (2017). Evaluation of density corrections to methane fluxes measured by open-path eddy covariance over contrasting landscapes. *Boundary-Layer Meteorology*, *165*(2), 197–210. https://doi.org/10.1007/s10546-017-0275-9

Chapple, D. E. (2017). *The influence of climate and seed dispersal on restoration in the San Francisco Bay*. UC Berkeley. Retrieved from https://escholarship.org/uc/item/9sx9k8z4

Chmura, G. L., Anisfeld, S. C., Cahoon, D. R., & Lynch, J. C. (2003). Global carbon sequestration in tidal, saline wetland soils. *Global Biogeochemical Cycles*, *17*(4), 1111. https://doi.org/10.1029/2002gb001917

Chu, H., Baldocchi, D. D., John, R., Wolf, S., & Reichstein, M. (2017). Fluxes all of the time? A primer on the temporal representativeness of FLUXNET. *Journal of Geophysical Research: Biogeosciences*, *122*(2), 289–307. https://doi.org/10.1002/2016JG003576

Chu, S. N., Wang, Z. A., Gonneea, M. E., Kroeger, K. D., & Ganju, N. K. (2018). Deciphering the dynamics of inorganic carbon export from intertidal salt marshes using high-frequency measurements. *Marine Chemistry*, *206*(July), 7–18. https://doi.org/10.1016/j.marchem.2018.08.005

Cloern, J. E., Canuel, E. A., & Harris, D. (2002). Stable carbon and nitrogen isotope composition of aquatic and terrestrial plants of the San Francisco Bay estuarine system. *Limnology & Oceanography*, *47*(3), 713–729. https://doi.org/10.4319/lo.2002.47.3.0713

Craft, C. B., Seneca, E. D., & Broome, S. W. (1993). Vertical accretion in microtidal regularly and irregularly flooded estuarine marshes. *Estuarine, Coastal and Shelf Science*, *37*, 371–386.

Crooks, S., Orr, M., Emmer, I., von Unger, M., Brown, B., & Murdiyarso, D. (2014). *Guiding principles for delivering coastal wetland carbon projects*. UNEP and CIFOR: United Nations Environment Programme. https://doi.org/10.17528/cifor/005210

Detto, M., Baldocchi, D. D., & Katul, G. G. (2010). Scaling properties of biologically active scalar concentration fluctuations in the atmospheric surface layer over a managed peatland. *Boundary-Layer Meteorology*, *136*(3), 407–430. https://doi.org/10.1007/s10546-010-9514-z

Deverel, S. J., Ingrum, T., & Leighton, D. (2016). Present-day oxidative subsidence of organic soils and mitigation in the Sacramento-San Joaquin Delta, California, USA. *Hydrogeology Journal*, *24*(3), 569–586. https://doi.org/10.1007/s10040-016-1391-1

Deverel, S. J., & Leighton, D. A. (2010). Historic, recent, and future subsidence, Sacramento-San Joaquin Delta, California, USA. *San Francisco Estuary and Watershed Science*, *8*(2), 1–24.

Deverel, S. J., Oikawa, P., Dore, S., Mack, S., & Silva, L. (2017). *The restoration of California deltaic and coastal wetlands*, version 1.1.

Drexler, J. Z. (2011). Peat formation processes through the millennia in tidal marshes of the Sacramento-San Joaquin Delta, California, USA. *Estuaries and Coasts*, *34*(5), 900–911. https://doi.org/10.1007/s12237-011-9393-7

Drexler, J. Z., Fontaine, C., & Wetlands, S. D. (2009). The legacy of wetland drainage on the remaining peat in the Sacramento—San Joaquin Delta, California, USA. *Wetlands*, *29*(1), 327–386.

Drexler, J. Z., Fontaine, C. S., & Brown, T. A. (2009). Peat accretion histories during the past 6,000 years in marshes of the Sacramento–San Joaquin Delta, CA, USA. *Estuaries and Coasts*, *32*(5), 871–892.

Drexler, J. Z., Khanna, S., Schoellhamer, D. H., & Orlando, J. (2018). The fate of blue carbon in the Sacramento-San Joaquin Delta of California, USA. In L. Windham-Myers, S. Crooks, & T. G. Troxler (Eds.), *A Blue carbon primer: The state of coastal wetland carbon science, practice, and policy* (1st ed., pp. 307–325). CRC Press.

Duarte, C. M., Losada, I. J., Hendriks, I. E., Mazarrasa, I., & Marbà, N. (2013). The role of coastal plant communities for climate change mitigation and adaptation. *Nature Climate Change*, *3*(11), 961–968. https://doi.org/10.1038/nclimate1970

Eichelmann, E., Hemes, K. S., Knox, S. H., Oikawa, P. Y., Chamberlain, S. D., Sturtevant, C., et al. (2018). The effect of land cover type and structure on evapotranspiration from agricultural and wetland sites in the Sacramento–San Joaquin River Delta, California. *Agricultural and Forest Meteorology*, *256–257*, 179–195. https://doi.org/10.1016/j.agrformet.2018.03.007

Emery, H. E., & Fulweiler, R. W. (2017). Incomplete tidal restoration may lead to persistent high CH_4 emission. *Ecosphere*, *8*(12). https://doi.org/10.1002/ecs2.1968

Emmer, I. M., Needelman, B. A., Emmett-Mattox, S., Crooks, S., Megonigal, J. P., Myers, D., et al. (2015). *Methodology for tidal Wetland and Seagrass restoration (VCS method)*. Verified Carbon Standard.

Evans, C. D., Peacock, M., Baird, A. J., Artz, R. R. E., Burden, A., Callaghan, N., et al. (2021). Overriding water table control on managed peatland greenhouse gas emissions. *Nature*. https://doi.org/10.1038/s41586-021-03523-1

Ewing, J. M., & Vepraskas, M. J. (2006). Estimating primary and secondary subsidence in an organic soil 15, 20, and 30 years after drainage. *Wetlands*, *26*(1), 119–130. https://doi.org/10.1672/0277-5212(2006)26[119:EPASSI]2.0.CO;2

Fennessy, S. M., & Lei, G. (2018). *Wetland restoration for climate change resilience. Ramsar briefing note No. 10. Gland, Switzerland: Ramsar convention secretariat*. Retrieved from www.ramsar.org

Forbrich, I., & Giblin, A. E. (2015). Marsh-atmosphere CO_2 exchange in a New England salt marsh. *Journal of Geophysical Research G: Biogeosciences*, *120*(9), 1825–1838. https://doi.org/10.1002/2015JG003044

Forbrich, I., Giblin, A. E., & Hopkinson, C. S. (2018). Constraining marsh carbon budgets using long-term c burial and contemporary atmospheric CO_2 Fluxes. *Journal of Geophysical Research: Biogeosciences*, *123*(3), 867–878. https://doi.org/10.1002/2017JG004336

Forster, P., Ramaswamy, V., Artaxo, P., Berntsen, T., Betts, R., Fahey, D. W., et al. (2007). Changes in atmospheric constituents and in radiative forcing. In S. Solomon, D. Qin, M. Manning, Z. Chen, M. Marquis, K. B. Averyt, et al. (Eds.), *Climate change 2007: The physical science basis. Contribution of working group I to the fourth assessment report of the intergovernmental panel on climate change* (pp. 228–237). Cambridge University Press. https://doi.org/10.20892/j.issn.2095-3941.2017.0150

Fregoso, T. A., Wang, R.-F., Alteljevich, E., & Jaffe, B. E. (2017). *San Francisco Bay-Delta bathymetric/topographic digital elevation model (DEM)*. U.S. Geological Survey. https://doi.org/10.5066/F7GH9G2

Gifford, R. M., & Roderick, M. L. (2003). Soil carbon stocks and bulk density: Spatial or cumulative mass coordinates as a basis of expression? *Global Change Biology*, *9*(11), 1507–1514. https://doi.org/10.1046/j.1365-2486.2003.00677.x

Glenn, E., Thompson, T. L., Frye, R., Riley, J., & Baumgartner, D. (1995). Effects of salinity on growth and evapotranspiration of Typha domingensis Pers. *Aquatic Botany*, *52*, 75–91.

Goals Project. (1999). *Baylands ecosystem habitat goals. A report of habitat recommendations prepared by the San Francisco Bay area wetlands ecosystem Goals project*. Goals Project.

Goals Project. (2015). *The baylands and climate change: What we can do. Baylands ecosystem habitat goals science update 2015*. Geomatica. San Francisco Bay Area Wetlands Ecosystem Goals project. California State Coastal Conservancy.

Gonneea, M. E., Maio, C. V., Kroeger, K. D., Hawkes, A. D., Mora, J., Sullivan, R., et al. (2019). Salt marsh ecosystem restructuring enhances elevation resilience and carbon storage during accelerating relative sea-level rise. *Estuarine, Coastal and Shelf Science*, *217*, 56–68. https://doi.org/10.1016/j.ecss.2018.11.003

Griscom, B. W., Adams, J., Ellis, P. W., Houghton, R. A., Lomax, G., Miteva, D. A., et al. (2017). Natural climate solutions. *Proceedings of the National Academy of Sciences*, *114*(44), 11645–11650. https://doi.org/10.1073/pnas.1710465114

Guo, H., Noormets, A., Zhao, B., Chen, J., Sun, G., Gu, Y., et al. (2009). Tidal effects on net ecosystem exchange of carbon in an estuarine wetland. *Agricultural and Forest Meteorology*, *149*(11), 1820–1828. https://doi.org/10.1016/j.agrformet.2009.06.010

Hammond, J. (2016). *San Francisco estuary invasive Spartina project California revegetation Program draft year 4 (2014–2015) installation report and year 5 (2015–2016) revegetation plan*.

Hatala, J. A., Detto, M., Sonnentag, O., Deverel, S. J., Verfaillie, J., & Baldocchi, D. D. (2012). Greenhouse gas (CO_2, CH_4, H_2O) fluxes from drained and flooded agricultural peatlands in the Sacramento-San Joaquin Delta. *Agriculture, Ecosystems & Environment*, *150*, 1–18. https://doi.org/10.1016/j.agee.2012.01.009

Hatala Matthes, J., Sturtevant, C., Oikawa, P. Y., Chamberlain, S. D., Szutu, D., Arias-Ortiz, A., et al. (2021). AmeriFlux BASE US-Myb Mayberry Wetland, Ver. 12-5, AmeriFlux AMP, (Dataset). *AmeriFlux AMP*. https://doi.org/10.17190/AMF/1246139

Heiri, O., Lotter, A. F., & Lemcke, G. (2001). Loss on ignition as a method for estimating organic and carbonate content in sediments: Reproducibility and comparability of results. *Journal of Paleolimnology*, *25*(1), 101–110. https://doi.org/10.1023/A:1008119611481

Hemes, K. S., Chamberlain, S. D., Eichelmann, E., Anthony, T., Valach, A., Kasak, K., et al. (2019). Agricultural and Forest Meteorology Assessing the carbon and climate benefit of restoring degraded agricultural peat soils to managed wetlands. *Agricultural and Forest Meteorology*, *268*, 202–214. https://doi.org/10.1016/j.agrformet.2019.01.017

Hemes, K. S., Chamberlain, S. D., Eichelmann, E., Knox, S. H., & Baldocchi, D. D. (2018). A biogeochemical compromise: The high methane cost of sequestering carbon in restored wetlands. *Geophysical Research Letters*, *45*(12), 6081–6091. https://doi.org/10.1029/2018GL077747

Hemes, K. S., Runkle, B. R. K., Novick, K. A., Baldocchi, D. D., & Field, C. B. (2021). An ecosystem-scale flux measurement strategy to assess natural climate solutions. *Environmental Science and Technology*, *55*(6), 3494–3504. https://doi.org/10.1021/acs.est.0c06421

Howard, J., Sutton-Grier, A., Herr, D., Kleypas, J., Landis, E., Mcleod, E., et al. (2017). Clarifying the role of coastal and marine systems in climate mitigation. *Frontiers in Ecology and the Environment*, *15*(1), 42–50. https://doi.org/10.1002/fee.1451

Ingebritsen, S., Ikehara, M. E., Galloway, D. L., & Jones, D. R. (2000). *Delta subsidence in California: The sinking heart of the state*.

IPCC. (2019). Summary for Policymakers. In H.-O. Pörtner, D. C. Roberts, V. Masson-Delmotte, P. Zhai, M. Tignor, E. Poloczanska, et al. (Eds.), *IPCC special report on the ocean and cryosphere in a changing climate*. In press.

Keller, J. (2018). Greenhouse gases. In L. Windham-Myers, S. Crooks, & T. G. Troxler (Eds.), *A blue carbon primer: The state of coastal wetland carbon science, practice, and policy* (1st ed., pp. 93–106). CRC Press. https://doi.org/10.1201/9780429435362

Kelley, C. A., Chanton, J. P., & Bebout, B. M. (2015). Rates and pathways of methanogenesis in hypersaline environments as determined by 13C-labeling. *Biogeochemistry*, *126*(3), 329–341. https://doi.org/10.1007/s10533-015-0161-9

Kirwan, M. L., & Megonigal, J. (2013). Tidal wetland stability in the face of human impacts and sea-level rise. *Nature*, *504*, 53–60.

Knox, S. H., Sturtevant, C., Matthes, J. H., Koteen, L., Verfaillie, J., & Baldocchi, D. (2015). Agricultural peatland restoration: Effects of land-use change on greenhouse gas (CO_2 and CH_4) fluxes in the Sacramento-San Joaquin Delta. *Global Change Biology*, *21*(2), 750–765. https://doi.org/10.1111/gcb.12745

Knox, S. H., Windham-Myers, L., Anderson, F., Sturtevant, C., & Bergamaschi, B. (2018). Direct and indirect effects of tides on ecosystem-scale CO_2 exchange in a brackish Tidal Marsh in Northern California. *Journal of Geophysical Research: Biogeosciences*, *123*(3), 787–806. https://doi.org/10.1002/2017JG004048

Krauss, K. W., Holm, G. O., Perez, B. C., McWhorter, D. E., Cormier, N., Moss, R. F., et al. (2016). Component greenhouse gas fluxes and radiative balance from two deltaic marshes in Louisiana: Pairing chamber techniques and eddy covariance. *Journal of Geophysical Research: Biogeosciences*, *121*(6), 1503–1521. https://doi.org/10.1002/2015JG003224

Kroeger, K. D., Crooks, S., Moseman-Valtierra, S., & Tang, J. (2017). Restoring tides to reduce methane emissions in impounded wetlands: A new and potent Blue Carbon climate change intervention. *Scientific Reports*, *7*(1), 11914. https://doi.org/10.1038/s41598-017-12138-4

Lynch, J., Cain, M., Pierrehumbert, R., & Allen, M. (2020). Demonstrating GWP: A means of reporting warming-equivalent emissions that captures the contrasting impacts of short- and long-lived climate pollutants. *Environmental Research Letters*, *15*(4). https://doi.org/10.1088/1748-9326/ab6d7e

Maher, D. T., Call, M., Santos, I. R., & Sanders, C. J. (2018). Beyond burial: Lateral exchange is a significant atmospheric carbon sink in mangrove forests. *Biology Letters*, *14*(7). https://doi.org/10.1098/rsbl.2018.0200

Maher, D. T., Santos, I. R., Golsby-Smith, L., Gleeson, J., & Eyre, B. D. (2013). Groundwater-derived dissolved inorganic and organic carbon exports from a mangrove tidal creek: The missing mangrove carbon sink? *Limnology & Oceanography*, *58*(2), 475–488. https://doi.org/10.4319/lo.2013.58.2.0475

Miller, R. L., Fram, M., Fujii, R., & Wheeler, G. (2008). Subsidence reversal in a re-established wetland in the Sacramento-San Joaquin Delta, California, USA. *San Francisco Estuary and Watershed Science*, *6*(3), 1–20. Retrieved from https://escholarship.org/uc/item/5j76502x

Mitsch, W. J., & Gossilink, J. G. (2000). The value of wetlands: Importance of scale and landscape setting. *Ecological Economics*, *35*(1), 25–33. https://doi.org/10.1016/S0921-8009(00)00165-8

Mitsch, W. J., Zhang, L., Waletzko, E., & Bernal, B. (2014). Validation of the ecosystem services of created wetlands: Two decades of plant succession, nutrient retention, and carbon sequestration in experimental riverine marshes. *Ecological Engineering*, *72*, 11–24. https://doi.org/10.1016/j.ecoleng.2014.09.108

Moffat, A. M., Papale, D., Reichstein, M., Hollinger, D. Y., Richardson, A. D., Barr, A. G., et al. (2007). Comprehensive comparison of gap-filling techniques for eddy covariance net carbon fluxes. *Agricultural and Forest Meteorology*, *147*(3–4), 209–232. https://doi.org/10.1016/j.agrformet.2007.08.011

Monaghan, M. C., Krishnaswami, S., & Turekian, K. K. (1986). The global-average production rate of 10Be. *Earth and Planetary Science Letters*, *76*(3–4), 279–287. https://doi.org/10.1016/0012-821X(86)90079-8

Morris, J. T., Sundareshwar, P. V., Nietch, C. T., Kjerfve, B., & Cahoon, D. R. (2002). Responses of coastal wetlands to rising sea level. *Ecology*, *83*(10), 2869–2877. https://doi.org/10.1890/0012-9658(2002)083[2869:ROCWTR]2.0.CO;2

Morton, R. A., & White, W. A. (1997). Characteristics of and corrections for core shortening in unconsolidated sediments. *Journal of Coastal Research*, *13*(3), 761–769.

Mount, J., & Twiss, R. (2005). Subsidence, Sea Level Rise, and Seismicity in the Sacramento–San Joaquin Delta. *San Francisco Estuary and Watershed Science*, *3*(1). https://doi.org/10.15447/sfews.2005v3iss1art7

Myhre, G., Shindell, D., Breón, F.-M., Collins, W., Fuglestvedt, J. S., Huang, J., et al. (2013). Anthropogenic and natural radiative forcing. In T. F. Stocker, D. Qin, G.-K. Plattner, M. Tignor, S. K. Allen, J. Boschung, et al. (Eds.), *Climate change 2013: The physical science basis. Contribution of working group I to the fifth assessment report of the intergovernmental panel on climate change*. Cambridge University Press. https://doi.org/10.3390/jmse6040146

Najjar, R. G., Herrmann, M., Alexander, R., Boyer, E. W., Burdige, D. J., Butman, D., et al. (2018). Carbon budget of tidal wetlands, estuaries, and shelf waters of Eastern North America. *Global Biogeochemical Cycles*, *32*(3), 389–416. https://doi.org/10.1002/2017GB005790

Needelman, B. A., Emmer, I. M., Emmett-Mattox, S., Crooks, S., Megonigal, J. P., Myers, D., et al. (2018). The science and policy of the verified carbon standard methodology for tidal wetland and seagrass restoration. *Estuaries and Coasts*, *41*(8), 2159–2171. https://doi.org/10.1007/s12237-018-0429-0

Neubauer, S. C. (2013). Ecosystem responses of a tidal freshwater marsh experiencing saltwater intrusion and altered hydrology. *Estuaries and Coasts*, *36*(3), 491–507. https://doi.org/10.1007/s12237-011-9455-x

Neubauer, S. C. (2014). On the challenges of modeling the net radiative forcing of wetlands: Reconsidering Mitsch et al. 2013. *Landscape Ecology*, *29*(4), 571–577. https://doi.org/10.1007/s10980-014-9986-1

Neubauer, S. C. (2021). Global warming potential is not an ecosystem property. *Ecosystems*. https://doi.org/10.1007/s10021-021-00631-x

Neubauer, S. C., & Megonigal, J. P. (2015). Moving beyond global warming potentials to quantify the climatic role of ecosystems. *Ecosystems*, *18*(6), 1000–1013. https://doi.org/10.1007/s10021-015-9879-4

Neubauer, S. C., & Verhoeven, J. T. A. (2019). Wetland effects on global climate: Mechanisms, impacts, and management recommendations. In S. An & J. T. A. Verhoeven (Eds.), *Wetlands: Ecosystem services, restoration and wise use* (pp. 39–62). Springer International Publishing. https://doi.org/10.1007/978-3-030-14861-4_3

Oikawa, P. Y. (2020). AmeriFlux BASE US-EDN eden landing ecological Reserve, ver. 2-5, AmeriFlux AMP, (Dataset). *AmeriFlux AMP*. https://doi.org/10.17190/AMF/1543381

OPC. (2018). *State of California rise guidance, 2018 update*. OPC.

Papale, D., Reichstein, M., Aubinet, M., Canfora, E., Bernhofer, C., Kutsch, W., et al. (2006). Towards a standardized processing of Net Ecosystem Exchange measured with eddy covariance technique: Algorithms and uncertainty estimation. *Biogeosciences*, *3*(4), 571–583. https://doi.org/10.5194/bg-3-571-2006

Petrescu, A. M. R., Lohila, A., Tuovinen, J. P., Baldocchi, D. D., Desai, A. R., Roulet, N. T., et al. (2015). The uncertain climate footprint of wetlands under human pressure. *Proceedings of the National Academy of Sciences of the United States of America*, *112*(15), 4594–4599. https://doi.org/10.1073/pnas.1416267112

Poffenbarger, H. J., Needelman, B. A., & Megonigal, J. P. (2011). Salinity influence on methane emissions from tidal marshes. *Wetlands*, *31*(5), 831–842. https://doi.org/10.1007/s13157-011-0197-0

Redfield, A. C. (1972). Development of a New England Salt Marsh. *Ecological Monographs*, *42*(2), 201–237. https://doi.org/10.2307/1942263

Robbins, J. A., & Edgington, D. N. (1975). Determination of recent sedimentation rates in Lake Michigan using Pb-210 and Cs-137. *Geochimica et Cosmochimica Acta*, *39*(3), 285–304. https://doi.org/10.1016/0016-7037(75)90198-2

Rogelj, J., & Schleussner, C. F. (2019). Unintentional unfairness when applying new greenhouse gas emissions metrics at country level. *Environmental Research Letters*, *14*(11). https://doi.org/10.1088/1748-9326/ab4928

Rosentreter, J. A., Borges, A. V., Deemer, B. R., Holgerson, M. A., Liu, S., Song, C., et al. (2021). Half of global methane emissions come from highly variable aquatic ecosystem sources. *Nature Geoscience*, *14*(4), 225–230. https://doi.org/10.1038/s41561-021-00715-2

Rosentreter, J. A., Maher, D. T., Erler, D. V., Murray, R. H., & Eyre, B. D. (2018). Methane emissions partially offset "blue carbon" burial in mangroves. *Science Advances*, *4*, eaao4985.

Sanchez-Cabeza, J. A., Masqué, P., & Ani-Ragolta, I. (1998). 210Pb and 210Po analysis in sediments and soils by microwave acid digestion. *Journal of Radioanalytical and Nuclear Chemistry*, *227*(1–2), 19–22. https://doi.org/10.1007/BF02386425

Sansone, F. J., Hollibaugh, J. T., Vink, S. M., Chambers, R. M., & Popp, B. N. (1994). Technical notes and comments diver-operated piston corer for nearshore use. *Estuaries*, *17*(3), 716–720.

Santos, I. R., Burdige, D. J., Jennerjahn, T. C., Bouillon, S., Cabral, A., Serrano, O., et al. (2021). The renaissance of Odum's outwelling hypothesis in "Blue Carbon" science. *Estuarine, Coastal and Shelf Science*, *255*, 107361. https://doi.org/10.1016/j.ecss.2021.107361

Santos, I. R., Maher, D. T., Larkin, R., Webb, J. R., & Sanders, C. J. (2019). Carbon outwelling and outgassing vs. burial in an estuarine tidal creek surrounded by mangrove and saltmarsh wetlands. *Limnology & Oceanography*, *64*(3), 996–1013. https://doi.org/10.1002/lno.11090

Sapkota, Y., & White, J. R. (2020). Carbon offset market methodologies applicable for coastal wetland restoration and conservation in the United States: A review. *The Science of the Total Environment*, *701*, 134497. https://doi.org/10.1016/j.scitotenv.2019.134497

Schäfer, K. V. R., Tripathee, R., Artigas, F., Morin, T. H., & Bohrer, G. (2014). Carbon dioxide fluxes of an urban tidal marsh in the Hudson-Raritan estuary. *Journal of Geophysical Research: Biogeosciences*, *119*, 2065–2081. https://doi.org/10.1002/2014JG002703

Siikamaki, J., Sanchirico, J. N., Jardine, S. L., Siikamäki, J., Sanchirico, J. N., & Jardine, S. L. (2012). Global economic potential for reducing carbon dioxide emissions from mangrove loss. *Proceedings of the National Academy of Sciences*, *109*(36), 14369–14374. https://doi.org/10.1073/pnas.1200519109

Stanford, B., Grossinger, R., Beagle, J., Askevold, R., Leidy, R., Beller, E., et al. (2013). *Alameda Creek watershed historical ecology study*.

Sturtevant, C., Ruddell, B. L., Knox, S. H., Verfaillie, J., Matthes, J. H., Oikawa, P. Y., & Baldocchi, D. (2016). Identifying scale-emergent, nonlinear, asynchronous processes of wetland methane exchange. *Journal of Geophysical Research: Biogeosciences*, *121*(1), 188–204. https://doi.org/10.1002/2015JG003054

Syvitski, J. P. M., Kettner, A. J., Overeem, I., Hutton, E. W. H., Hannon, M. T., Brakenridge, G. R., et al. (2009). Sinking deltas due to human activities. *Nature Geoscience*, *2*(10), 681–686. https://doi.org/10.1038/ngeo629

Taillardat, P., Ziegler, A. D., Friess, D. A., Widory, D., Truong Van, V., David, F., et al. (2018). Carbon dynamics and inconstant porewater input in a mangrove tidal creek over contrasting seasons and tidal amplitudes. *Geochimica et Cosmochimica Acta*, *237*, 32–48. https://doi.org/10.1016/j.gca.2018.06.012

Valach, A. C., Kasak, K., Hemes, K. S., Anthony, T. L., Dronova, I., Taddeo, S., et al. (2021). Productive wetlands restored for carbon sequestration quickly become net CO_2 sinks with site-level factors driving uptake variability. *PLoS One*, *16*(3 March), 1–22. https://doi.org/10.1371/journal.pone.0248398

Valach, A. C., Kasak, K., Hemes, K. S., Szutu, D., Verfaillie, J., & Baldocchi, D. D. (2021). Carbon flux trajectories and site conditions from restored impounded marshes in the Sacramento-San Joaquin Delta. In K. W. Krauss, Z. Zhu, & C. L. Stagg (Eds.), *Wetland carbon and environmental management* (pp. 247–271). https://doi.org/10.1002/9781119639305.ch13

Valach, A. C., Szutu, D., Eichelmann, E., Knox, S., Verfaillie, J., & Baldocchi, D. D. (2021). AmeriFlux BASE US-Tw1 Twitchell Wetland West Pond, Ver. 9-5, AmeriFlux AMP, (Dataset). *AmeriFlux AMP*. https://doi.org/10.17190/AMF/1246147

Vroom, J., Wegen, M. van der, Martyr-Koller, R. C., & Lucas, L. V. (2017). What determines water temperature dynamics in the San Francisco Bay-Delta System? *Water Resources Research*, *53*(11), 9901–9921. https://doi.org/10.1002/2016WR020062

Wang, Z. A., & Cai, W. J. (2004). Carbon dioxide degassing and inorganic carbon export from a marsh-dominated estuary (the Duplin River): A marsh CO_2 pump. *Limnology & Oceanography*, *49*(2), 341–354. https://doi.org/10.4319/lo.2004.49.2.0341

Wang, Z. A., Kroeger, K. D., Ganju, N. K., Gonneea, M. E., & Chu, S. N. (2016). Intertidal salt marshes as an important source of inorganic carbon to the coastal ocean. *Limnology & Oceanography*, *61*(5), 1916–1931. https://doi.org/10.1002/lno.10347

Watson, E. B., & Byrne, R. (2009). Abundance and diversity of tidal marsh plants along the salinity gradient of the San Francisco Estuary: Implications for global change ecology. *Plant Ecology*, *205*(1), 113–128. https://doi.org/10.1007/s11258-009-9602-7

Webb, J. R., Santos, I. R., Maher, D. T., & Finlay, K. (2018). The importance of aquatic carbon fluxes in net ecosystem carbon budgets: A catchment-scale review. *Ecosystems*, 1–20. https://doi.org/10.1007/s10021-018-0284-7

Wendt, J. W., & Hauser, S. (2013). An equivalent soil mass procedure for monitoring soil organic carbon in multiple soil layers. *European Journal of Soil Science*, *64*(1), 58–65. https://doi.org/10.1111/ejss.12002

Windham-Myers, L., Cai, W. J., Alin, S., Andersson, A., Crosswell, J., Dunton, K., et al. (2018). Tidal wetlands and estuaries. In N. Cavallaro, G. Shrestha, R. Birdsey, M. A. Mayes, R. G. Najjar, S. C. Reed, et al. (Eds.), *Second state of the carbon cycle report (SOCCR2): A sustained assessment report* (pp. 596–648). U.S. Global Change Research Program. https://doi.org/10.7930/SOCCR2.2018.CH15

Windham-Myers, L., Stuart-Haëntjens, E., Bergamaschi, B., Knox, S., Anderson, F., & Nakatsuka, K. (2020). *FLUXNET-CH4 US-srr suisun marsh - rush ranch*. https://doi.org/10.18140/FLX/1669694

Xie, X., Zhang, M. Q., Zhao, B., & Guo, H. Q. (2014). Dependence of coastal wetland ecosystem respiration on temperature and tides: A temporal perspective. *Biogeosciences*, *11*(3), 539–545. https://doi.org/10.5194/bg-11-539-2014

Zhou, J., Theroux, S. M., Bueno de Mesquita, C. P., Hartman, W. H., Tian, Y., & Tringe, S. G. (2021). Microbial drivers of methane emissions from unrestored industrial salt ponds. *The ISME Journal*, (July), 1–12. https://doi.org/10.1038/s41396-021-01067-w